Physica 19D (1986) 89–111
North-Holland, Amsterdam

STEADY SOLUTIONS OF THE KURAMOTO–SIVASHINSKY EQUATION

Daniel MICHELSON*
The Hebrew University of Jerusalem, Institute of Mathematics and Computer Science, Givat Ram, 91904 Jerusalem, Israel and University of California at Los Angeles, Department of Mathematics, CA 90024, USA

Steady solutions of the Kuramoto–Sivashinsky equation are studied. These solutions are defined on the whole x line and propagate with a constant speed c^2 in time. For large c^2 it is shown that the solution is unique and has a conical form. For small c^2 there is a periodic solution and an infinite set of quasi-periodic solutions as asserted by Moser's twist map theorem. Numerical computations for intermediate values of c^2 suggest that below $c^2 \approx 1.6$ for every speed there is a continuum of odd quasi-periodic solutions or a Cantor set of chaotic solutions wrapped by infinite sequences of conic solutions.

Received 14 September 1984
Revised manuscript received 8 July 1985

1. Introduction

The Kuramoto–Sivashinsky equation

$$u_t + \nabla^4 u + \nabla^2 u + \tfrac{1}{2}|\nabla u|^2 = 0, \quad u = u(x,t) \tag{1.1}$$

has attracted for the last decade a considerable attention [1–12]. It was originally derived by Kuramoto and Tsuzuki [1] in the context of a reaction diffusion system, and by Sivashinsky [5] in the context of flame front propagation. In the later case $u(x,t)$ represents the perturbation of a plane flame front which propagates in a fuel–oxygen mixture. Numerical experiments [2, 3, 6] have shown that eq. (1.1) when solved on a sufficiently large interval $-l < x < l$ with periodic boundary conditions tends to a turbulent state as $t \to \infty$. The solution $u(x,t)$ has the form

$$u(x,t) = -c_0^2 t + v(x,t), \tag{1.2}$$

where $c_0^2 \approx 1.2$ is a universal constant independent of the initial condition, while the mean value of $v(x,t)$ is close to zero. For a fixed t the function $v(x,t)$ although irregular has an appearance of a quasi-periodic wave with a characteristic wave length $l_0 = 2\pi/\omega_0$, $\omega_0 = \sqrt{2}/2$. Note that the frequency ω_0 is maximally amplified by the linear terms in (1.1). Formula (1.2) suggests that one should look for steady solutions of (1.1)

$$u(x,t) = -c^2 t + v(x). \tag{1.3}$$

Clearly $v(x)$ satisfies the O.D.E.

$$\frac{d^4 v}{dx^4} + \frac{d^2 v}{dx^2} = c^2 - \frac{1}{2}\left(\frac{dv}{dx}\right)^2 \tag{1.4}$$

or a third order equation for the derivative $y = dv/dx$

$$\frac{d^3 y}{dx^3} + \frac{dy}{dx} = c^2 - \frac{1}{2}y^2, \quad -\infty < x < +\infty. \tag{1.5}$$

The main objective of this work is to study the set of bounded solutions of (1.5) and its dependence on the parameter c.

For large c we shall show that eq. (1.5) has a unique (up to translation) bounded solution. This solution $y(x)$ is an odd function of x, tends to the limits $\lim_{x\to\pm\infty} y(x) = \mp c\sqrt{2}$ and vanishes only at $x = 0$. The integral $v(x) = \int_0^x y(\tau)\,d\tau$ has thus a

*This work was supported by an Alfred Sloan Foundation Fellowship and the National Science Foundation under Grant No. MCS 78-01252.

0167-2789/86/$03.50 © Elsevier Science Publishers B.V.
(North-Holland Physics Publishing Division)

conical form with a single maximum at $x=0$ and slopes $\pm\sqrt{2}\,c$ as $x\to\mp\infty$. The above function $v(x)$ has a following physical interpretation. A slight modification of (1.1),

$$u_t+\nabla^4 u+\nabla^2 u+\tfrac{1}{2}|\nabla u|^2=c^2, \tag{1.6}$$

is a model equation (due to Sivashinsky) for a conical flame front with a slope $c\sqrt{2}$ on a Bunsen burner. Clearly, the above $v(x)$ represents a stationary flame on a Bunsen burner.

For small c eq. (1.5) has a periodic solution y_{per} with frequency ω depending on c. It turns out that the Poincaré map associated with the periodic solution is measure preserving and satisfies for small c the conditions of Moser's twist map theorem [14]. As a result, the flow defined by (1.5) possesses an infinite set of coelecial invariant tori surrounding the periodic orbit. The boundaries of the tori are closures of quasi-periodic orbits. We show that the integrals of these quasi-periodic solutions are quasi-periodic too. This results in an infinite set of quasi-periodic solutions of (1.4).

The periodic solution y_{per} as well as ω and c could be expanded in power series with respect to an auxiliary parameter ε. The numerical computation of these series reveals that the periodic solution exists up to $c_{\max}\approx 1.26606$. The complete ω, c curve is displayed on fig. 1. The part P_0P_2Q of the graph corresponds to the domain where the analytic expansion is valid. The portion QP_5P_8 was calculated using a difference approximation to (1.5). The branch $P_4P_6'P_8'$ represents a non-odd periodic solution bifurcating from the point P_4. This branch could be continued until the limit point $\omega=0$, $c\approx 0.86$ which corresponds to an "oblique" soliton (see figs. 4c–4e). The periodic orbits are parabolic at the points P_i, P_i', and elliptic and hyperbolic at the segments indicated by letters e and h respectively. In the elliptic regions the Moser's twist map theorem applies so that there are infinitely many invariant tori.

A central difference approximation of (1.5) was used in order to compute the bounded odd solutions for intermediate values of c. The results suggest that for $c>c_1\approx 1.3$ there is only one such

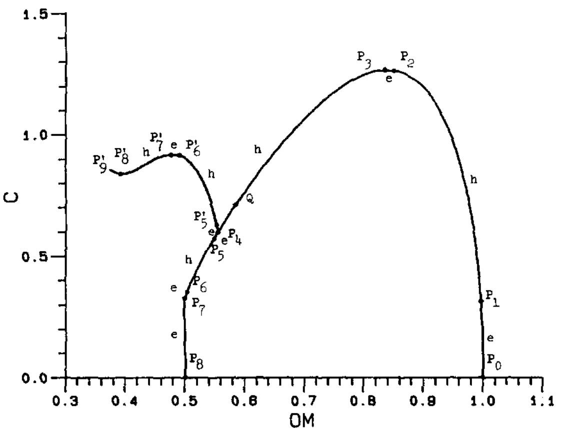

Fig. 1. The ω–c curve for the periodic solution. The branch $P_4P_7'P_9'$ corresponds to the non-odd periodic solution.

solution. In the interval $c_{\max}<c\le c_1$, there is a decreasing sequence of bifurcation points $c_1, c_2, \ldots, c_n\to c_{\max}$. At $c=c_n$ a new solution $y_n(x)$ is "born" which splits into two solutions as c decreases. The function $y_n(x)$ tends to the critical points $\pm c\sqrt{2}$ as $x\to\mp\infty$ and has n zeros in the half line $x>0$. Thus the integral $v_n(x)=\int_0^x y_n(\tau)\,d\tau$ would correspond to a Bunsen flame with $n+1$ maxima. At $c=c_{\max}$ the above solutions tend to the periodic one as $n\to\infty$. For $c<c_{\max}$ the set of odd bounded solutions (of the scheme) is quite complicated. The basic form of the solutions is determined by the periodic orbits. In the elliptic domains there are invariant tori while in the hyperbolic domains there exists a Cantor-type set of chaotic solutions which "float" around the periodic ones. On the other hand for all values of c below $c_{\max}$ (at least up to $c=0.2$ there exist infinite sequences of odd asymptoti solutions (i.e. connecting the critical points). Thes sequences of "Bunsen flame" type solutions lie i the "holes" of the Cantor set and approximate th above chaotic solutions.

2. Topological properties of the set of bounded solutions

First we shall prove that for any closed interva $c\in[0,c_*]$ the sets of all bounded solutions of (1.5

are uniformly bounded. Rewrite (1.5) as a first order system

$$\frac{d\bar{y}}{dx} = f(\bar{y}, c) = \left(y_2, y_3, c^2 - y_2 - \tfrac{1}{2}y_1^2\right),$$
$$\bar{y} = (y_1, y_2, y_3). \quad (2.1)$$

At that point it is worthwhile to consider a more general situation of a system

$$\frac{dy}{dx} = f(y), \quad -\infty < x < \infty, \quad (2.2)$$

where $y = (y^{(1)}, \ldots, y^{(N)}) \in \mathrm{R}^N$, $f = (f^{(1)}, \ldots, f^{(N)}) \in \mathrm{R}^N$ and $f(y)$ is a smooth vector function, say $f \in \mathrm{C}^1(\mathrm{R}^N)$. Assume that

$$f(y) = h(y) + g(y), \quad (2.3)$$

where $h(y)$ is a "pseudo-homogeneous" leading part of $f(y)$. Namely, there exists a positive real vector $s = (s_1, s_2, \ldots, s)$ and real scalar r such that

$$\rho^r \rho^{-s} h(\rho^s y) = h(y) \quad (2.4)$$

and

$$\rho^r \rho^{-s} g(\rho^s y) \to 0 \quad \text{as} \quad \rho \to 0,$$
$$\text{uniformly for} \quad |y| \le 1. \quad (2.5)$$

Here

$$\begin{aligned} \rho^s y &= \left(\rho^{s_1} y^{(1)}, \rho^{s_N} y^{(N)}\right), \\ \rho^r \rho^{-s} h &= \left(\rho^r \rho^{-s_1} h^{(1)}, \ldots, \rho^r \rho^{-s_N} h^{(N)}\right) \end{aligned} \quad (2.6)$$

and similarly in (2.5).

Assume that the leading system

$$\frac{dy}{dx} = h(y) \quad (2.7)$$

does not have bounded solution for $-\infty < x < \infty$ but $y = 0$.

Lemma 2.1. Under the above assumptions the set of bounded solutions of (2.2) is uniformly bounded in the maximum norm.

Proof. Assume to the contrary that there exists a sequence of bounded solutions $y_n(x)$ such that $\sup_x |y_n(x)| \to \infty$. Introduce the norm $\|y\| = \sum_{i=1}^{N} |y^{(i)}|^{1/s_i}$. Without loss we may assume that

$$\|y_n(0)\| = \rho_n \to \infty \quad \text{and} \quad \sup_x \|y_n(x\|/\rho_n \le 2. \quad (2.8)$$

Change the variables $z = \rho_n^{-s} y$, $\xi = \rho_n^{-r} x$. Then the function $z_n(\xi)$ satisfies the equations

$$\frac{dz_n}{d\xi} = \varphi_n(z_n) = h(z_n) + \rho_n^r \rho_n^{-s} g(\rho_n^s z_n), \quad (2.9)$$

while

$$\|z_n(0)\| = 1 \quad \text{and} \quad \sup_\xi \|z_n(\xi)\| \le 2. \quad (2.10)$$

Clearly, in the bounded set $\|z\| \le 2$ the term $\rho^r \rho^{-s} g(\rho^s z)$ tends uniformly to 0 as $\rho \to \infty$. Since $\|z_n(\xi)\|$ and $\|dz_n(\xi)/d\xi\|$ are uniformly bounded, there exists a subsequence of $z_n(\xi)$ which converges uniformly on any finite interval to a bounded solution $z(\xi)$ of the equation $dz/d\xi = h(z)$. In view of (2.10) $\|z(0)\| = 1$ which contradicts our assumption about the system (2.7).

Lemma 2.1 obviously applies to system (2.1) with $h(\bar{y}) = (y_2, y_3, -\tfrac{1}{2}y_1^2)$, $s = (1, 4/3, 5/3)$ and $r = -1/3$. The system $d\bar{y}/dx = h(\bar{y})$ is equivalent to the single equation $y''' = -\tfrac{1}{2}y^2$ for $y = y_1$. One can easily show that the last equation does not have bounded solutions. Although the function f in (2.1) depends on a parameter c, it is clear that in a compact domain of y and c variables, the function $g(\bar{y}) = (0, 0, c^2 - y_2)$ satisfies the condition of (2.5).

For $c \gg 1$ change in (1.5) the variables

$$z = y/(c\sqrt{2}), \quad \xi = x(c\sqrt{2})^{1/3}. \quad (2.11)$$

Eq. (1.5) then becomes

$$\frac{d^3 z}{d\xi^3} + \varepsilon \frac{dz}{d\xi} = \frac{1}{2}(1 - z^2), \quad \varepsilon = (c\sqrt{2})^{-2/3} \ll 1 \quad (2.12)$$

or as a system

$$\frac{\mathrm{d}\bar{z}}{\mathrm{d}\xi} = \left(z_2, z_3, \tfrac{1}{2}\left(1 - z_1^2\right) - \varepsilon z_2\right), \quad \bar{z} = (z_1, z_2, z_3). \tag{2.13}$$

Again, as in system (2.1), the set of the bounded solutions of (2.13) for ε in a compact interval $\varepsilon \in [0, \varepsilon_*]$ is uniformly bounded.

Our next step is to show that the Conley index of the set of all bounded solutions of (2.1) is zero. Let us recall briefly (for details see [17]) some properties of this index.

a) Conley's index is a homotopy type of a pointed topological space.

b) For each isolated invariant set of a flow there is a corresponding index.

c) The index of a disjoint union of isolated invariant sets of a flow is a sum of their indices (i.e., the homotopy type of the wedge of the corresponding pointed topological spaces).

d) The index of an isolated invariant set does not change under a homotopy of the flow (provided the invariant set remains isolated under the homotopy).

e) The index of a hyperbolic critical point or of a hyperbolic periodic orbit is non-zero.

The flow in (2.1) could be extended by a two parameter homotopy

$$\frac{\mathrm{d}\bar{y}}{\mathrm{d}x} = \left(y_2, y_3, t - sy_2 - \tfrac{1}{2}y_1^2\right), \qquad t \in [-c^2, c^2], s \in [0,1] \tag{2.14}$$

to

$$\frac{\mathrm{d}\bar{y}}{\mathrm{d}x} = \left(y_2, y_3, -c^2 - \tfrac{1}{2}y_1^2\right).$$

The last system does not have bounded solutions (see [17], p. 12). Denote by $I(t, s)$ the set of all bounded solutions of (2.2). Again as in (2.1) $I(t, s)$ is uniformly bounded (and thus isolated) for t and s as in (2.14). Since the index of $I(-c^2, 0) = \varnothing$ is zero, so is the index of $I(t, s)$. Note that for $t > 0$ system (2.14) has two critical points $\bar{y}_\mathrm{L} = (\sqrt{2t}, 0, 0)$ and $\bar{y}_\mathrm{R} = -\bar{y}_\mathrm{L}$, which are both hyperbolic. Thus we have proved

Theorem 2.1. Critical points or hyperbolic periodic orbits may not be isolated components of the set of bounded solutions of (2.14) for $t > 0$.

Now we consider eq. (1.5) for large c or equivalently (2.13) for small $\varepsilon > 0$. For $\varepsilon = 0$ system (2.13) was firstly studied in [18] (see also [19] and [17]). Clearly it has a non-trivial bounded solution. Since there is Liapunov function $L(\bar{z}) = z_2 z_3 - z_1/2 + z_1^3/6$, the above solution connects the critical points. Recently McCord [20] has shown that there is only one non-trivial bounded solution. Hence the solution is odd, i.e. $z = z_1(x)$ is an odd function. Moreover, $z_1(x)$ vanishes only at 0 and $\mathrm{d}z_1/\mathrm{d}x(0) < 0$. It is then easy to show that the two dimensional stable manifold $M_\mathrm{st}(\bar{z}_\mathrm{R})$ of the critical point $\bar{z}_\mathrm{R} = (-1,0,0)$ and the unstable two-dimensional manifold $M_\mathrm{u}(\bar{z}_\mathrm{L})$ of the critical point $\bar{z}_\mathrm{L} = -\bar{z}_\mathrm{R}$ intersect transversally along the above bounded solution. We claim that the same results hold also for small $\varepsilon \neq 0$. Namely,

Theorem 2.2. There exists a constant $\varepsilon_0 > 0$ such that for all $|\varepsilon| < \varepsilon_0$ system (2.13) has one and only one (up to translation) bounded solution $\bar{z}(x; \varepsilon)$. This solution connects the critical points $\bar{z}_\mathrm{L}$ and $\bar{z}_\mathrm{R}$, $z_1(x; \varepsilon)$ is an odd function of x and vanishes only at $x = 0$.

Proof. The transversality implies that for small ε system (2.13) has a bounded solution $\bar{z}(x; \varepsilon)$ which is close to $\bar{z}(x; 0)$ and connects the critical points. Moreover we may assume that $\bar{z}(0; \varepsilon) = 0$ and that $\bar{z}(x; \varepsilon) \neq 0$ for $x \neq 0$. In order to prove uniqueness suppose by contrary that there is a sequence $\varepsilon_n \to$ and corresponding non-trivial bounded solution $\bar{z}_n(x)$ and $\bar{z}_n'(x)$ of (2.13) so that $\bar{z}_n'$ is not a shift of $\bar{z}_n$. Since the above solutions are uniformly bounded, without loss we may assume that both sequences $\bar{z}_n$ and $\bar{z}_n'$ converge uniformly on finite intervals to the solution $\bar{z}(x; 0)$. As it follows from lemma 2.2 below, for sufficiently large n the solutions $\bar{z}_n$ and $\bar{z}_n'$ connect the critical points $\bar{z}_\mathrm{L}$ and $\bar{z}_\mathrm{R}$ and thus the corresponding unstable and stable manifolds intersect along two close trajectories

This, however, contradicts the transversality of the intersection for $\varepsilon = 0$. Thus it remains to prove

Lemma 2.2. Let $\bar{z}_n(x)$ be a sequence of bounded solutions of system (2.13). Suppose that $\bar{z}_n(x)$ converges uniformly on bounded intervals to $\bar{z}(x;0)$ as $\varepsilon = \varepsilon_n \to 0$. Then for sufficiently large n, $\lim_{x \to -\infty} \bar{z}_n(x) = \bar{z}_{\mathrm{L}} = (1,0,0)$, $\lim_{x \to \infty} \bar{z}_n(x) = \bar{z}_{\mathrm{R}} = (-1,0,0)$.

Proof. First observe that for any neighborhood U_{R} of $\bar{z}_{\mathrm{R}}$ which is disjoint with $\bar{z}_{\mathrm{L}}$ there exist $\varepsilon_0 > 0$ and a neighborhood $U_{\mathrm{R}}' \subset U_{\mathrm{R}}$ of $\bar{z}_{\mathrm{R}}$ such that for $|\varepsilon| \le \varepsilon_0$ any bounded solution of (2.13) which belongs to U_{R}' for some $x = x_0$ will stay in U_{R} for $x > x_0$. Indeed, otherwise there exists sequence $\varepsilon_n \to 0$ and corresponding sequence of bounded solutions $\bar{z}_n(x)$ so that $\bar{z}_n(x_0) \to \bar{z}_{\mathrm{R}}$, $\bar{z}_n(x_n) \notin U_{\mathrm{R}}$ for some $x_n > x_0$ and $\bar{z}_n(x) \in U_{\mathrm{R}}$ for $x_0 \le x < x_n$. By uniform boundedness of $\bar{z}_n(x)$ we may assume that $\bar{z}_n(x_n)$ converges to $\bar{z}_* \in \mathrm{R}^3 \setminus U_{\mathrm{R}}$. Clearly $\bar{z}_*$ belongs to the bounded trajectory $\bar{z}(x;0)$. Note that $x_n \to \infty$ since otherwise $\bar{z}_*$ would be connected with $\bar{z}_{\mathrm{R}}$ in backward direction by $\bar{z}(x;0)$. Now, leaving $\bar{z}_*$ by the trajectory $\bar{z}(x;0)$ in backward direction we should reach in a finite time T a small neighborhood U_{L} of $\bar{z}_{\mathrm{L}}$. By continuity, for large n also $\bar{z}_n(x_n - T) \in U_{\mathrm{L}}$. However $x_n - T > x_0$ for large n and therefore $\bar{z}_n(x_n - T) \in U_{\mathrm{R}}$. Hence a contradiction. Now, for sufficiently small U_{R} and ε any solution of (2.13) which stays in U_{R} in forward time will tend to $\bar{z}_{\mathrm{R}}$. We choose a corresponding U_{R}' and a small ε_0, and similarly for the point $\bar{z}_{\mathrm{L}}$. Select T such that $\bar{z}(-T;0) \in U_{\mathrm{L}}'$ and $\bar{z}(T;0) \in U_{\mathrm{R}}'$. Then for sufficiently large n, $\bar{z}_n(-T)$ and $\bar{z}_n(T)$ belong to the above neighborhoods and thus $\bar{z}_n$ connects the critical points. Q.E.D.

We conclude this section with the following observation:

Lemma 2.3. Let $\bar{y}(x)$ be a bounded solution of (2.1) such that $\bar{y}(x)$ has no limit as $x \to +\infty(x \to -\infty)$. Then $+\infty(-\infty)$ is an accumulation point of the zeros of $y_1(x)$.

Proof. Indeed, otherwise $y_1(x)$ is of a constant sign for x greater than some x_0. The function $L(\bar{y}) = y_3^2 + y_2^2 + y_1^2 y_2 - 2c^2 y_2$ is then a Liapunov function of (2.1) for $x > x_0$ since $\mathrm{d}L(\bar{y})/\mathrm{d}x = 2y_1 y_2^2$, and therefore $\bar{y}(x)$ has a limit at $+\infty$.

3. Periodic and quasi-periodic solutions for $c \ll 1$.

Consider eq. (1.5) for $0 < c \ll 1$. As in [9] we are looking for periodic solutions with frequency $\omega = 1 + \mathcal{O}(c)$. It is convenient to rescale the variables so that the period is independent of c. Introduce

$$\xi = \omega x, \quad z = y/\omega^3. \tag{3.1}$$

Then

$$\frac{\mathrm{d}^3 z}{\mathrm{d}\xi^3} + \lambda \frac{\mathrm{d}z}{\mathrm{d}\xi} = \varepsilon^2 - \frac{z^2}{2}, \tag{3.2}$$

where

$$\varepsilon = c/\omega^3, \quad \lambda = \omega^{-2} = 1 + \mathcal{O}(\varepsilon). \tag{3.3}$$

Periodic solution of (3.2) with period 2π could be found by means of a power expansion in ε

$$z_{\mathrm{per}} = \sum_{n=1}^{\infty} z_n(\xi)\varepsilon^n, \quad \lambda = 1 + \sum_{n=1}^{\infty} \lambda_n \varepsilon^n. \tag{3.4}$$

Substitution of (3.4) into (3.2) gives

$$\begin{aligned} &z_1''' + z_1' = 0, \quad z_2''' + z_2' = 1 - \lambda_1 z_1' - z_1^2/2, \\ &z_3''' + z_3' = -\lambda_1 z_2' - \lambda_2 z_1' - z_1 z_2, \quad \text{etc.} \end{aligned} \tag{3.5}$$

Thus $z_1 = b_{10} + a_{11}\sin\xi + b_{11}\cos\xi$. Shifting ξ one may always assume that $b_{11} = 0$. In order to avoid resonance in the equation for z_2 one should assume that $\lambda_1 = 0$, $b_{10}\, a_{11} = 0$ and $b_{10}^2/2 + a_{11}^2/4 = 1$. Here there are two possibilities. If $a_{11} = 0$ then $b_{10} = \pm\sqrt{2}$ and we recover the stationary solution $z \equiv \pm\varepsilon\sqrt{2}$. If $b_{10} \equiv 0$, then $a_{11} = \pm 2$ and as it follows from consequent equations,

$$z_n(\xi) = \sum_{k=1}^{n} a_{nk} \sin k\xi, \tag{3.6}$$

so that $z_{\mathrm{per}}(\xi)$ is an odd function. The solutions with $a_{11} = +2$ an $a_{11} = -2$ are related by the shift $\xi \to \xi + \pi$. Let us select $a_{11} = -2$ so that for small $\varepsilon > 0$, $z'(0) < 0$. The first two terms of the expansion are

$$\begin{aligned} z_{\mathrm{per}} &= -2\varepsilon \sin \xi - \tfrac{1}{6}\varepsilon^2 \sin 2\xi + \mathcal{O}(\varepsilon^3), \\ \lambda &= 1 + \varepsilon^2/12 + \mathcal{O}(\varepsilon^4). \end{aligned} \tag{3.7}$$

Actually all $\lambda_{2n+1} = 0$ and $a_{nk} = 0$ if $n - k$ is odd. The expansion in (3.4) could be justified rigorously using the Liapunov–Shmidt reduction. Namely, a periodic solution of (3.2) with period 2π may be expanded as

$$z_{\mathrm{per}}(\xi) = b_0 + a_1 \sin \xi + \left[\sum_{n=2}^{\infty} a_n \sin n\xi + \sum_{n=2}^{\infty} b_n \cos n\xi \right]. \tag{3.8}$$

(Shifting ξ if necessary we may assume that there is no $\cos \xi$ in the expansion.) Let H be the Hilbert space of functions as in (3.8) with scalar product $\langle u, v\rangle = \int_0^{2\pi} (u'''\bar{v}''' + u\bar{v}) \mathrm{d}x$ and $H_1 = L_2[0, 2\pi]$. We consider the mapping

$$F\colon (z, \mu, \varepsilon) \to z''' + (1+\mu)z' - \varepsilon^2 + z^2/2 \tag{3.9}$$

as a mapping from $H \oplus \mathbb{C} \oplus \mathbb{C}$ into H_1. Clearly F is differentiable and even analytic. Denote by $\tilde{H} \subset H_1$ and $\tilde{H}_1 \subset H_1$ the subspaces spanned by $\sin n\xi$, $\cos n\xi$, $n \geq 2$ and let $P\colon H \to \tilde{H}$, $P_1\colon H_1 \to \tilde{H}_1$ be the corresponding orthogonal projectors. Consider the map

$$\tilde{F} = P_1 \circ F\colon H \oplus \mathbb{C} \oplus \mathbb{C} \to \tilde{H}_1. \tag{3.10}$$

Note that the differential $\mathrm{d}\tilde{F}(0)$ at zero when restricted to the subspace $\tilde{H}$ is an isomorphism. Thus the implicit map theorem applies and the equation $\tilde{F}(z, \mu, \varepsilon) = 0$ could be solved as

$$\begin{aligned} Pz = \tilde{z} &= \sum_{n=2}^{\infty} a_n \sin n\xi + \sum_{n=2}^{\infty} b_n \cos n\xi = f(b_0, a_1, \mu \\ &= f_a(b_0, a_1, \mu) + f_b(b_0, a_1, \mu), \end{aligned} \tag{3.11}$$

where f_a represents the first sum in $\tilde{z}$ and f_b the second one. Note that b_0, a_1 and μ enter $\tilde{F}$ only through quadratic terms. Therefore

$$\mathrm{d}f(0) = 0. \tag{3.12}$$

Next, the map $\tilde{F}$ vanishes for all constant $z = b_0$. Therefore

$$f(b_0, 0, \mu) = 0. \tag{3.13}$$

Finally, $F(z(\xi), \mu, \varepsilon) = F(-z(-\xi), \mu, \varepsilon)$, and hence for $b_0 = 0$

$$f_b(0, a_1, \mu) \equiv 0. \tag{3.14}$$

In view of (3.13) and (3.14) and the analyticity of

$$\begin{aligned} f_a(b_0, a_1, \mu) &= a_1 f_a'(b_0, a_1, \mu), \\ f_b(b_0, a_1, \mu) &= a_1 b_0 f_b'(b_0, a_1, \mu), \end{aligned} \tag{3.15}$$

where the maps f_a' and f_b' are analytic. By (3.12 also

$$f_a'(0) = 0. \tag{3.16}$$

Now consider the remaining equations $(I - P_1) \circ$ $= 0$. They are

$$\mu a_1 - \tfrac{1}{2} \sum_{n=1}^{\infty} a_n a_{n+1} - \tfrac{1}{2} \sum_{n=2}^{\infty} b_n b_{n+1} = 0 \tag{3.17}$$

for $\cos \xi$ component,

$$-b_0 a_1 - \tfrac{1}{2} \sum_{n=2}^{\infty} (a_{n+1} - a_{n-1}) b_n = 0 \tag{3.18}$$

for $\sin \xi$ component and

$$-\varepsilon^2 + \tfrac{1}{4} \sum_{n=1}^{\infty} a_n^2 + \tfrac{1}{4} \sum_{n=2}^{\infty} b_n^2 + \tfrac{1}{2} b_0^2 = 0 \tag{3.19}$$

for the constant component.

If $a_1 = 0$, by (3.13) and (3.19) we obtain the trivial solution $z = \varepsilon\sqrt{2}$. Now let a_1 be small and different from 0. We will show that $b_0 = 0$. Indeed, otherwise divide (3.18) by $b_0 a_1$. Then

$$1 + \tfrac{1}{2}a_1\left[\sum_{n-2}^{\infty}(a'_{n+1} - a'_{n-1})b'_n\right] = 0, \tag{3.20}$$

where $a'_n = a_n/a_1$, $b'_n = b_0/a_1 b_0$. In view of (3.15) the expression in the brackets in (3.20) is an analytic function of a_1, b_0 and μ. However, a_1 is small and thus (3.20) is impossible. It then follows from (3.14) that all $b_n = 0$. Then from (3.17) we recover

$$\mu = \tfrac{1}{2}a_1\sum_{n=1}^{\infty} a'_n a'_{n+1} = a_1 f_\mu(a_1, \mu), \tag{3.21}$$

where f_μ is an analytic function. By the implicit function theorem (3.21) could be solved for μ:

$$\mu = a_1\varphi_\mu(a_1). \tag{3.22}$$

Finally, eq. (3.19) is used to compute a_1,

$$a_1^2\left(1 + \sum_{n=2}^{\infty}(a'_n)^2\right) = 4\varepsilon^2. \tag{3.23}$$

Since by (3.16) $\Sigma_{n=2}^{\infty}(a'_n)^2 = \mathcal{O}(a_1^2)$ we get for small ε

$$a_1 = \pm 2\varepsilon + \mathcal{O}(\varepsilon^3) \tag{3.24}$$

and then by (3.22) and (3.11) recover z and $\lambda = 1 + \mu$ as analytic functions of ε.

Using a computer, we have calculated the first 100 terms of the expansion in (3.4). The radius of convergence is

$$|\varepsilon| \le R \approx 3.558.$$

By (3.3) one can also reconstruct the values of ω and c corresponding to ε. The ω, c curve is shown on fig. 1. The maximal $c = c_{\max} \approx 1.266$ corresponds to $\omega \approx 0.84$. The frequency $\omega_0 = \sqrt{2}/2$, as mentioned in the Introduction, is maximally amplified by the linear terms in (1.1). The corresponding value of $c^2 = 1.17$ in the graph is close to the mean propagation velocity $c_0^2 \approx 1.2$ of a turbulent flame as calculated by the numerical experiment in [6]. The portion of the ω, c curve on fig. 1 extending from P_0 through P_1, P_2, P_3 to Q corresponds to the above domain of convergence $|\varepsilon| \le R$. For ε close to R one cannot rely any more on computations based on 100 terms of the expansion in (3.4). To circumvent this difficulty, we approximate (1.5) by a difference scheme in (4.1) and compute instead the periodic solutions of the scheme. The entire graph on fig. 1 is actually based on such computation with a step size Δx in (4.1) being l/N where $l = l(c)$ is the period of the solution and $N = 120$ is the number of grid points in the period. The periodic solution is found by following the fixed point of a corresponding Poincaré map, while the fixed points are computed using Newton's method. One should note that an expansion as in (3.4) exists also for the periodic solution of the difference scheme. We found that for $N = 120$ the periodic solutions for the difference and differential equation in the domain P_0Q differ by less than 0.5%. The points P_i, P'_i on the graph are parabolic points, i.e. the eigenvalues of the Jacobian of the Poincaré map at these points are $\lambda_1 = \lambda_2 = -1$ or $\lambda_1 = \lambda_2 = 1$. At $P_1, P_2, P_5, P_6, P'_5, P'_6$ the eigenvalues are $\lambda_1 = \lambda_2 = -1$ while at P_3, P_4, P'_7 and P'_8 they are $\lambda_1 = \lambda_2 = 1$. In all cases the Jacobian has a single eigenvector. At P_7 the periodic solution coincides as a double loop with the one at P_1 and follows (as a double loop) the branch P_1P_0 until the endpoint P_8! Thus, for the same values of c the frequency ω at the branch P_7P_8 is half the one at the branch P_1P_0. In the neighborhood of P_4 we were surprised to find another fixed point of the Poincaré map corresponding to non-odd periodic solution. This solution branches out at P_4 and continues through the points P'_5, P'_6, P'_7, P'_8. By symmetricity, $-y(-x)$ would be another non-odd solution. The values of ω and c at the parabolic points appear on table I. Our computations show that the variable $\varepsilon = c/\omega^3$ grows monotonically as one moves along the ω, c

Table I
The values of c and ω at the parabolic points

Parab. points	P_1	P_2	P_3	P_4	P_5	P_6	P_7	P_5'	P_6'	P_7'	P_8'
c	0.3195	1.2660	1.2664	0.5982	0.5796	0.3407	0.3195	0.606	0.9165	0.917	0.8365
ω	0.9961	0.8424	0.8372	0.5548	0.5502	0.5012	0.4981	0.554	0.479	0.477	0.393
Eigenvalues	−1	−1	1	1	−1	−1	1	−1	−1	1	1

curve from P_0 towards Q and reaches its maximum at the point Q. Another experimental observation is that the coefficients λ_n of the expansion in (3.4) are positive. Hence at Q, ε equals the radius of convergence R and $\mathrm{d}\lambda/\mathrm{d}\varepsilon$ is infinite there. We need the above arguments since a direct computation of the singular point of $\lambda(\varepsilon)$ using, a reasonable number of terms in (3.4) is too inaccurate.

Our next goal is to study the Poincaré map $\mathscr{P}$ associated with the periodic solution z_{per} in (3.7). Change in (3.2) the variable

$$z \to z/\varepsilon \tag{3.25}$$

and rewrite the corresponding equation as a system

$$\frac{\mathrm{d}\bar{z}}{\mathrm{d}\xi} = f(\bar{z}, \varepsilon) = \left(z', z'', \varepsilon - \varepsilon z^2/2 - \lambda(\varepsilon) z'\right),$$
$$\bar{z} = (z, z', z''). \tag{3.26}$$

The plane $z'' = 0$ intersects the periodic trajectory $\bar{z}_{\text{per}}$ at least at two points $\bar{z}_0 = (0, z'_{\text{per}}(0), 0)$ and $\bar{z}_1 = (0, z'_{\text{per}}(\pi), 0)$. (We use the old notation z_{per} for the rescaled $z_{\text{per}}/\varepsilon$). Denote by R^2 the plane $z'' = 0$, by $D^2 \subset R^2$ a small disk centered at $\bar{z}_0$ and by $\mathscr{P}$: $D^2 \to R^2$ the corresponding Poincaré map. Observe that the flow in (3.26) is volume preserving since $\operatorname{div} f(\bar{z}, \varepsilon) = 0$. Hence the map $\mathscr{P}$ preserves the measure $(\varepsilon - \varepsilon z^2/2 - \lambda(\varepsilon) z')\,\mathrm{d}z\,\mathrm{d}z'$. As far as $z'_{\text{per}}(0) < 0$ this measure is positive in a neighborhood of $\bar{z}_0$. For small ε, $z'_{\text{per}}(0) = -2 + \mathcal{O}(\varepsilon) < 0$. Our computations show that $z'_{\text{per}}(0)$ remains negative along the whole curve on fig. 1. Besides the volume preservation, the flow in (3.26) is invariant under the change of variables $(z, z', z'') \to (-z, z', -z'')$, $\xi \to -\xi$. As a result $\mathscr{P}$ satisfies the identity

$$J\mathscr{P} = \mathscr{P}^{-1} J, \tag{3.27}$$

where $J = J^{-1}$: $\mathrm{R}^2 \to \mathrm{R}^2$ maps the pair (z, z') into $(-z, z')$. Consider the differential $\mathrm{d}\mathscr{P}(\bar{z}_0)$ of the map $\mathscr{P}$ at $\bar{z}_0$. Clearly,

$$|\det \mathrm{d}\mathscr{P}(\bar{z}_0)| = 1. \tag{3.28}$$

In order to compute $\mathrm{d}\mathscr{P}(\bar{z}_0)$ one should solve the linearized equation

$$z''' + \lambda(\varepsilon) z' = -\varepsilon z_{\text{per}} z. \tag{3.29}$$

Expand

$$z = z_1 + \varepsilon z_2 + \mathcal{O}(\varepsilon^2). \tag{3.30}$$

Then,

$$z_1''' + z_1' = 0, \quad z_2''' + z_2' = 2 \sin \xi \cdot z_1, \tag{3.31}$$

so that

$$z = a_1(1 - \varepsilon\xi \sin \xi) + a_2\left(\sin \xi + \varepsilon\xi + \varepsilon \frac{\sin 2\xi}{6}\right)$$
$$+ a_3\left(\cos \xi + \varepsilon \frac{\cos 2\xi}{6}\right) + \mathcal{O}(\varepsilon^2). \tag{3.32}$$

Now we impose conditions on a_3 and $\xi = 2\pi + \Delta$ so that

$$z''(0) = 0,$$
$$z''_{\text{per}}(2\pi + \Delta\xi) + z''(2\pi + \Delta\xi) = \mathcal{O}(\Delta\xi^2). \tag{3.3}$$

Thus

$$a_3 = -2a_1\varepsilon + \mathcal{O}(\varepsilon^2) \tag{3.3}$$

and

$$\Delta\xi = -z''(2\pi)/\left(z'''_{\text{per}}(2\pi) + z'''(2\pi)\right) = \mathcal{O}(\varepsilon^2). \tag{3.35}$$

The transformation $\mathrm{d}\mathscr{P}(\bar{z}_0)$ is defined by

$$\begin{aligned}\mathrm{d}\mathscr{P}(\bar{z}_0)&: (z(0), z'(0))\\ &\to \left(z(2\pi) + \Delta\xi\, z'_{\text{per}}(0), z'(2\pi) + \Delta\xi\, z''_{\text{per}}(0)\right).\end{aligned} \tag{3.36}$$

An easy computation shows that

$$\mathrm{d}\mathscr{P}(\bar{z}_0) = I + 2\pi\varepsilon\begin{pmatrix} 0 & 1 \\ -1 & 0\end{pmatrix} + \mathcal{O}(\varepsilon^2). \tag{3.37}$$

For small ε the eigenvalues of $\mathrm{d}\mathscr{P}(\bar{z}_0)$ are

$$\lambda_{1,2} = \mathrm{e}^{\pm\mathrm{i}\alpha_0(\varepsilon)}, \quad \alpha_0(\varepsilon) = 2\pi\varepsilon + \mathcal{O}(\varepsilon^2), \tag{3.38}$$

i.e. they are complex conjugate and on the unit circle. Thus for small ε the periodic solution is elliptic. This domain of ellipticity extends until the point P_1 (see fig. 1). The other elliptic domains are P_2P_3, P_4P_5, P_6P_7 and P_7P_8 (the last one coincides with P_0P_1). At the bifurcating branch of the non-odd periodic solution the elliptic domains are $P_4P'_5$ and $P'_6P'_7$. In the elliptic regions one would expect the existence of nested invariant tori surrounding the periodic orbit. In order to prove it rigorously, one should verify the conditions of Moser's twist map theorem (e.g. see [13], pp. 225–228). First recall that the map $\mathscr{P}$ depends analytically on z and z' in a small neighborhood D^2 and preserves the positive measure $(\varepsilon - \lambda(\varepsilon)z' - \varepsilon z^2/2)\,\mathrm{d}z\,\mathrm{d}z'$. Next we should compute the Birkhoff normal form of $\mathscr{P}$ (see [13], pp. 158–159). For small ε this could be done analytically. Change the variables

$$\delta z = z, \quad \delta z' = z' - z'_{\text{per}}(0). \tag{3.39}$$

In the new variables the Poincaré map $\mathscr{P}$ depends analytically on δz, $\delta z'$ and ε in a neighborhood of 0. Our computations (see the appendix) show that

$$\begin{aligned}\mathscr{P}(\delta z, \delta z'; \varepsilon) &= \mathrm{d}\mathscr{P}(\delta z, \delta z'; \varepsilon)\\ &\quad + \mathrm{d}^2\mathscr{P}(\delta z, \delta z'; \varepsilon) + \mathcal{O}(\varepsilon^2),\end{aligned} \tag{3.40}$$

i.e. the higher differentials with respect to δz and $\delta z'$ are of order $\mathcal{O}(\varepsilon^2)$, and

$$\begin{aligned}&\mathrm{d}\mathscr{P}(\delta z, \delta z'; \varepsilon)\\ &\quad = \left[I + 2\pi\varepsilon\begin{pmatrix} 0 & 1 \\ -1 & 0\end{pmatrix} + \mathcal{O}(\varepsilon^2)\right]\begin{pmatrix}\delta z \\ \delta z'\end{pmatrix},\end{aligned} \tag{3.41}$$

$$\begin{aligned}&\mathrm{d}^2\mathscr{P}(\delta z, \delta z'; \varepsilon)\\ &\quad = \varepsilon\pi\begin{pmatrix} -(\delta z)^2 - (\delta z')^2/2 \\ \delta z\cdot\delta z'\end{pmatrix} + \mathcal{O}(\varepsilon^2).\end{aligned} \tag{3.42}$$

Then a quadratic change of variables (see the appendix)

$$\begin{aligned}\delta z &= \frac{1}{2\mathrm{i}}(u - \bar{u}) + \mathcal{O}(\varepsilon),\\ \delta z' &= \tfrac{1}{2}(u + \bar{u}) - \tfrac{1}{16}(u^2 - 6u\bar{u} + \bar{u}^2) + \mathcal{O}(\varepsilon)\end{aligned} \tag{3.43}$$

brings $\mathscr{P}$ to the form

$$\mathscr{P}: (u, \bar{u}) \to (u_1, \bar{u}_1), \quad u_1 = \mathrm{e}^{\mathrm{i}\alpha}u + \varepsilon^2\mathcal{O}(|u|^4), \tag{3.44}$$

where

$$\begin{aligned}\alpha &= \alpha_0(\varepsilon) + \alpha_1(\varepsilon)u\bar{u}, \quad \alpha_0(\varepsilon) = 2\pi\varepsilon + \mathcal{O}(\varepsilon^2),\\ \alpha_1(\varepsilon) &= -\frac{3\pi}{8}\varepsilon + \mathcal{O}(\varepsilon^2).\end{aligned} \tag{3.45}$$

Thus for small $\varepsilon > 0$

$$\alpha_1(\varepsilon) \neq 0 \quad \text{and} \quad n\alpha_0(\varepsilon) \neq 0 (\operatorname{mod} 2\pi), \qquad \text{for } 1 \le n \le 4, \tag{3.46}$$

and the conditions of the twist map theorem have been verified. The result implied by the theorem is as follows:

There exist numbers $r_0 > 0$ and $\varepsilon_0 > 0$ such that for any $\varepsilon \in (0, \varepsilon_0)$ and any $\omega \in (\alpha_0(\varepsilon), \alpha_0(\varepsilon) + \alpha_1(\varepsilon)r_0^2)$ satisfying infinitely many inequalities

$$\left|\frac{\omega}{2\pi} - \frac{p}{q}\right| \ge \beta q^{-\tau} \tag{3.47}$$

with some positive β, τ and all integers $q > 0$, p, *there exists an invariant curve S of $\mathscr{P}$ of the form*

$$S\colon\ \delta z=\delta z(\varphi),\quad \delta z'=\delta z'(\varphi),\quad z''=0,\quad \varphi\in\mathrm{R}. \tag{3.48}$$

The functions $\delta z(\varphi)$ and $\delta z'(\varphi)$ are periodic with period 2π and depend analytically on φ. The curve in (3.48) *is a perturbation of order $r\varepsilon$ of a circle*

$$\delta z=-r\sin\varphi,\quad \delta z'=r\cos\varphi,$$
$$r=\left[\frac{16}{3}\left(1-\frac{\omega}{2\pi\varepsilon}\right)\right]^{1/2} \tag{3.49}$$

and the map induced by $\mathscr{P}$ on the curve is

$$\varphi\to\varphi+\omega. \tag{3.50}$$

The solutions of (3.26) which originate at the curve (3.48) form a two-dimensional torus $\mathscr{T}$ and for $-\infty<\xi<\infty$ each trajectory on the torus is everywhere dense in $\mathscr{T}$. We shall show that the above solutions are quasi-periodic functions of ξ. Let $\mathscr{N}$ be a small tubular neighborhood of the periodic solution $\bar z_{\text{per}}(\xi;\varepsilon)$. One can parametrize $\mathscr{N}$ in the longitudinal direction by a parameter $\vartheta\in[0,2\pi]$ so that

a) $e^{i\vartheta}$ is an analytic function of $\bar z\in\mathscr{N}$ and $\varepsilon\in[-\varepsilon_0,\varepsilon_0]$;

b) $\vartheta\equiv 0 \pmod{2\pi}$ at the section $z''=0$ in a neighborhood of $\bar z_0$;

c) $\vartheta(\bar z_{\text{per}}(\xi;\varepsilon))=\xi\in[0,2\pi]$.

To do this, one could for example define a reper

$$e_1(\xi;\varepsilon)=\mathrm{d}\bar z_{\text{per}}(\xi;\varepsilon)/\mathrm{d}\xi,$$
$$e_2(\xi;\varepsilon)=\mathrm{d}^2\bar z_{\text{per}}(\xi;\varepsilon)/\mathrm{d}\xi^2,\quad e_3=e_1\times e_2.$$

For small ε these vectors are independent. If $\bar n(0)$ is a unit vector normal to the plane $z''=0$ and $\bar n(0)=\sum\alpha_i(\varepsilon)e_i(0;\varepsilon)$, define

$$\bar n(\xi;\varepsilon)=\sum\alpha_i(\varepsilon)e_i(\xi;\varepsilon).$$

Now let ϑ satisfy (c) and be constant along the sections

$$\left(\bar z-\bar z_{\text{per}}(\xi;\varepsilon)\right)\cdot\bar n(\xi;\varepsilon)=0.$$

Then for small $|\varepsilon|$ and $\mathscr{N}$, ϑ is defined uniquely and satisfies the above conditions. Now we introduce on $\mathscr{T}$ global analytic coordinates (φ,ϑ), $\varphi\in[0,2\pi]$, $\vartheta\in[0,2\pi]$ such that the trajectories of (3.26) on $\mathscr{T}$ are described by

$$\varphi=\varphi_0+(\omega/2\pi)\vartheta(\operatorname{mod}2\pi). \tag{3.51}$$

Along a trajectory, parameters ξ and ϑ are related by the equation

$$\frac{\mathrm{d}\xi}{\mathrm{d}\vartheta}=g(\vartheta,\varphi;\varepsilon),\quad \frac{\mathrm{d}\varphi}{\mathrm{d}\vartheta}=\omega/2\pi, \tag{3.52}$$

where $g(\vartheta,\varphi;\varepsilon)$ is analytic in ϑ, φ and ε and periodic in ϑ,φ with period 2π. In view of the conditions in (3.47), ξ could be written as

$$\xi=\beta_0\vartheta+h_0(\vartheta), \tag{3.53}$$

where $\beta_0=(2\pi)^{-2}\int_0^{2\pi}\int_0^{2\pi}g(\vartheta,\varphi;\varepsilon)\,\mathrm{d}\vartheta\,\mathrm{d}\varphi$ and $h_0(\vartheta)$ is a quasi-periodic function of the class $\mathrm{Q}(1,\omega/2\pi)$ (see [13], pp. 258–264). Note that for small $\mathscr{N}$ and ε, $g(\vartheta,\varphi;\varepsilon)\approx 1$ and $\mathrm{d}\xi/\mathrm{d}\vartheta$ is bounded away from 0. Thus the inverse function is

$$\vartheta=\beta_0^{-1}\xi+h_1(\xi), \tag{3.54}$$

where $h_1(\xi)$ is quasi-periodic and belongs to the class $\mathrm{Q}(\beta_0^{-1},\beta_0^{-1}\omega/2\pi)$. Since $\bar z$ is a periodic function of φ, ϑ, the trajectory $\bar z(\xi)$ is a quasi-periodic function of ξ of the class $\mathrm{Q}(\beta_0^{-1},\beta_0^{-1}\omega/2\pi)$.

Finally we will show that the integral

$$w(\xi)=\int_{\tau=0}^{\xi}z(\tau)\,\mathrm{d}\tau \tag{3.55}$$

is quasi-periodic too.Consider the invariant curve in (3.48). We may assume that $\delta z(0)=0$. As it follows from (3.27), the curve

$$\varphi\to(-\delta z(-\varphi),\delta z'(-\varphi)) \tag{3.56}$$

is also invariant under $\mathscr{P}$. By uniqueness $\delta z(n\omega)=-\delta z(-n\omega)$ and $\delta z'(n\omega)=\delta z'(-n\omega)$ for all $n\in\mathbb{Z}$. Hence

$$\delta z(\varphi)=-\delta z(-\varphi),\quad \delta z'(\varphi)=\delta z'(-\varphi). \tag{3.57}$$

Let $\bar{z}(\xi)$ be a trajectory of (3.26) which originates (when $\xi = 0$) at the point $(\delta z(\varphi), \delta z'(\varphi), z'' = 0)$ and let $\tau(\varphi)$ be the value of ξ as the trajectory reaches the point $(\delta z(\varphi + \omega), \delta z'(\varphi + \omega), z'' = 0)$. Denote $g(\varphi) = \int_0^{\tau(\varphi)} z(\xi)\,d\xi$. Clearly, $g(\varphi)$ is an analytic function of φ with period 2π. Observe that $(-z(-\xi), z'(-\xi), -z''(-\xi))$ is a trajectory of (3.26) which connects the points $(\delta z(-\varphi - \omega), \delta z'(-\varphi - \omega), z'' = 0)$ and $(\delta z(-\varphi), \delta z'(-\varphi), z'' = 0)$ as ξ changes from $-\tau(\varphi)$ to 0. Hence

$$g(-\varphi - \omega) = \int_{-\tau(\varphi)}^{0} -z(-\xi)\,d\xi = -g(\varphi),$$

and consequently

$$\int_0^{2\pi} g(\varphi)\,d\varphi = 0. \tag{3.58}$$

As a result of (3.58) and (3.47) the sums

$$\sum_{n=0}^{N} g(\varphi + n\omega) \tag{3.59}$$

are uniformly bounded. This implies that the average

$$\lim_{\xi \to \infty} \frac{1}{\xi} \int_0^{\xi} z(\tau)\,d\tau = 0. \tag{3.60}$$

Hence $w(\xi)$ is a quasi-periodic function of the class $Q(\beta_0^{-1}, \beta_0^{-1}\omega/2\pi)$. Recall that the function $w(\xi)$ is proportional to $v(x)$ in (1.3). Thus, we have proved the existence of slowly propagating quasi-periodic flame fronts (in Sivashinsky's model). These waves have the basic frequency of order 1, and a modulation with an incommensurable frequency of order $\omega/2\pi$.

Moser's twist map theorem tells us that the relative measure of the invariant tori in $\mathcal{N}$ tends to 1 as $\mathcal{N}$ shrinks to the periodic orbit. The domains bounded by each pair of (coelecial) tori is invariant under the flow. Besides the quasi-periodic solutions there is also an infinite set of periodic solutions which is everywhere dense in $\mathcal{N}$. The frequency ω of periodic solutions (which is a rational number) lies in the range $(\alpha_0(\varepsilon), \alpha_0(\varepsilon) + \alpha_1(\varepsilon)r_0^2)$. It is quite possible that for some periodic solutions the average in (3.60) is non-zero and the corresponding integral in (3.55) has a non-zero slope.

4. Numerical experiments

In order to gather more information about the set of bounded solutions of (1.5), especially for intermediate values of c, we have approximated (1.5) by a difference equation and solved it on a computer. The difference scheme employed was

$$(y_{j+3} - 3y_{j+2} + 3y_{j+1} - y_j)/\Delta x^3 + (y_{j+2} - y_{j+1})/\Delta x = c^2 - \tfrac{1}{4}(y_{j+2}^2 + y_{j+1}^2), \quad j \in \mathbb{Z}, \tag{4.1}$$

where y_j is the value of the grid function at $x_j = j\Delta x$. The scheme in (4.1) maintains the symmetry of the equation in (1.5) in the sense that it is invariant under the transformation

$$j \to -j, \quad y \to -y. \tag{4.2}$$

We have investigated mainly the odd solutions of (4.1), i.e. those which satisfy the initial conditions

$$y_0 = 0, \quad y_1 = -y_{-1} = \Delta x \cdot s, \tag{4.3}$$

where s is a parameter. The values of y_j, $j \geq 2$ are then calculated by (4.1) until $|y_j|$ exceed a certain large number $y_{\max}$. Denote by $x_{\max}(s)$ the point $x_j = j\Delta x$ where for the first time $|y_j| \geq y_{\max}$. Recall that for $c \in [0, c_0]$ all bounded solutions of (1.5) lay in a strip $|y| \leq y_{\max}$ where $y_{\max}$ depends only on c_0. The same is true for eq. (4.1). Thus for bounded solutions $x_{\max}(s) = \infty$. It was a surprising empirical observation that with a few exceptions all local maxima of $x_{\max}(s)$ have been infinite. Hence a sequence $s_1 < s_2 < s_3$ with non-monotone $x_{\max}(s_i)$ would imply that for some $s \in [s_1, s_3]$ the corresponding solution is bounded. Of course one cannot be sure that there is only one bounded solution. Hence the interval was subdivided into, say, 100 subintervals, and if no additional maxima appeared, it was assumed that there is only one bounded solution. Then a Golden Section method for a univalent function was employed in order to converge to above s. As suggested by the theory in sections 2 and 3, only solutions connecting the critical points were isolated. Since these solutions are asymptotically unstable, in order to reach $x_{\max} \approx 100$ the double precision on CDC (i.e. 30 decimal digits) was required. We set $y_{\max} = 10$, $\Delta x \approx 0.05$ and considered c in the interval $[0,4]$. The results are as follows. For $c > c_1 \approx 1.283$ problem (4.1), (4.3) has a single bounded solution. This solution corresponds to $s < 0$, vanishes only at $j = 0$ and tends to the critical points. We followed this solution until $c = 0.2$. As c decreased, the above solution did not change its shape, i.e. vanished only at $j = 0$, until we reached $c \approx 0.3$. Then additional zero point evolved which split in two as c decreased below 0.3. At $c = 0.2$ our solution was almost unseparable from an invariant tori. At $c = c_1 \approx 1.283$ a bifurcation occurs. A new bounded solution $y_j^{(1)}$ with a slope $s_1 > 0$ is born. This solution has exactly one zero for $j > 0$ (i.e. one change of sign) and connects the critical points. For $c < c_1$, $y_j^{(1)}$ splits into two similar solutions $y_j^{(1)}$ and $y_j^{(-1)}$ with slopes s_1 and s_{-1}. At $c = c_2 \approx 1.274$ a second bifurcation occurs where another solution $y_j^{(2)}$ with a slope $s_2 < 0$ is formed. For $c < c_2$, $y_j^{(2)}$ splits into $y_j^{(2)}$ and $y_j^{(-2)}$ with slopes $s_2, s_{-2} < 0$. Both $y_j^{(2)}$ and $y_j^{(-2)}$ have exactly 2 zeros in the domain $j < 0$. As c decreases, at $c = c_3 \approx 1.2679$ and $c = c_4 \approx 1.2673$ solutions $y_j^{(3)}$ and $y_j^{(4)}$ are formed with correspondingly 3 and 4 zeros in the half line $j < 0$. On the other hand eq. (4.1) like (1.5) has periodic solution. Namely, for $\Delta x(0) = 2\pi/N$, N integer, there exist analytic functions $\Delta x = \Delta x(\varepsilon)$, $c = c(\varepsilon)$ and periodic grid function $y_j^{(\mathrm{per})}(\varepsilon)$, $j \in \mathbb{Z}$ with $y_j^{(\mathrm{per})}(\varepsilon) = y_{j+N}^{(\mathrm{per})}(\varepsilon)$ which satisfy (4.1). We have computed, the above functions for $N = 120$. The graph of $c(\varepsilon)$ versus the discrete frequency $\omega(\varepsilon) = 2\pi/(N\Delta x(\varepsilon))$ is almost the same as for the periodic solution of (1.5). In particular, the maximal value $c_{\max}$ of $c(\varepsilon)$ is 1.2664 instead of 1.2662 for the differential problem. Our computations at $c = c_{\max}$ with the corresponding $\Delta x = \Delta x(\varepsilon) \approx 0.0625$ show that the set of *odd* bounded solutions of (4.1) consists of two sequences $\{y_j^{(n)}\}$ and $\{y_j^{(-n)}\}$, $n = 0,1,2,\ldots$ with slopes s_n and s_{-n} and a periodic solution $y_j^{(\mathrm{per})}$. The functions $y_j^{(n)}$ and $y_j^{(-n)}$ have n zeros (i.e. changes of sign) in the domain $j > 0$, and tend to the critical points $\pm c_{\max} \cdot \sqrt{2}$. The slope s_n is positive for n odd and negative for n even. The sequences s_{2n} and s_{2n+1}, $n > 0$ are decreasing, s_{-2n}, s_{-2n-1} are increasing. The limits $s_{\mathrm{ev}} = \lim s_{2n} = \lim s_{-2n}$ and $s_{\mathrm{od}} = \lim s_{2n+1} = \lim s_{-2n-1}$ are the slopes of the periodic solution $y^{(\mathrm{per})}$ corresponding to $c_{\max}$ at $j = 0$ and at $j = N/2$. The functions $y_j^{(2n)}$ thus tend to $y_j^{(\mathrm{per})}$ while $y_j^{(2n+1)}$ tend to $y_{j+N/2}^{(\mathrm{per})}$. The above statement is indeed a conjecture which is based on actual computation of $y_j^{(\pm n)}$ for $|n| \le 20$ and $x_j \le 80$–90. On an interval $0 \le x \le 80$–90 we observe about 20–25 local extrema of the function $y_j^{(n)}$. Note that the condition $x_{\max}(s) > 90$ sometimes determines s up to 25 significant digits! Based on the above results we also conjecture that there is a sequence of bifurcation points c_n which tends monotonically to $c_{\max}$. At $c = c_n$ the solution $y_j^{(n)}$ is born and splits into $y_j^{(n)}$ and $y_j^{(-n)}$ as c decreases beyond c_n. On fig. 2 the solutions $y_j^{(0)}$, $y_j^{(1)}$, $y_j^{(-1)}$, $y_j^{(3)}$ and $y_j^{(\mathrm{per})}$ at $c = c_{\max}$ are displayed. We followed $y_j^{(0)}$ until $c = 0.2$ and $y_j^{(-2)}$ and $y_j^{(-4)}$ until $c = 0.3$ (see figs. 10 and 11). The solution $y_j^{(-4)}$ disappeared somewhere between $c = 0.3$ and $c = 0.295$ while $y_j^{(-2)}$ disappeared between $c = 0.295$ and $c = 0.293$. We conjecture that each solution $y_j^{(n)}$ exists until some c_n'. At $c = c_n'$, $y_j^{(n)}$ becomes a limit of a sequence of bounded oscillating solutions and disappears for $c < c_n'$.

As c decreases beyond $c_{\max} \approx 1.26644$, there is sudden change in the set of bounded solution. The periodic solution splits into two. The elliptic one is surrounded by a thin invariant torus. As c decreases from $c_{\max}$ to $c \approx 1.26603$ at the parabolic point P_2 (fig. 1), the thickness of the maximal tori measured by the slope s first increases from 0 to 2×10^{-3} and then decreases back to 0. By the

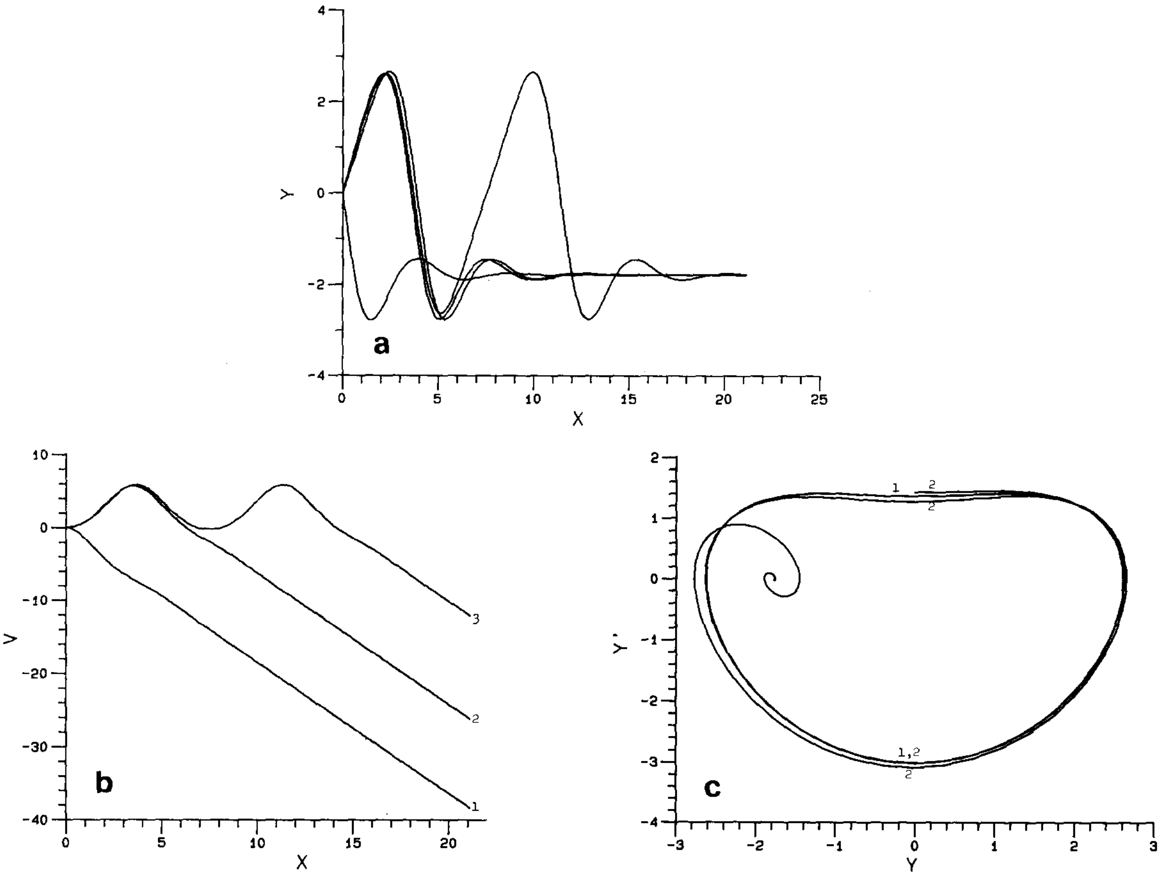

Fig. 2(a) $c = c_{max} \approx 1.266$, asymptotic solutions $y^{(0)}$, $y^{(1)}$, $y^{(-1)}$ and $y^{(3)}$. (b) $c = c_{max}$, curves 1, 2, 3 represent the Bunsen flames corresponding to the solutions $y^{(0)}, y^{(1)}, y^{(3)}$. (c) $c = c_{max}$, curves 1 and 2 correspond to the solutions y_{per} and $y^{(3)}$.

rem 2.1 the hyperbolic periodic solution may not be isolated from other bounded solutions. Denote by I the set of slopes s corresponding to the bounded odd solutions of (4.1). At $c = 1.2663$ (i.e. between the points P_3 and P_2) the set I is as follows. First, I splits into two parts I_1 and I_2, where I_1 is concentrated near $s = -3.0275$ and I_2 near $s = 1.36$. These are approximately the slopes of periodic solutions at $\xi = 0$ and $\xi = \pi$. The lower bound of I_1 is $s_0 \approx -3.1567$, the upper bound is $s_2 \approx -3.0111$. These slopes correspond to solutions $y^{(0)}$ and $y^{(2)}$ above. The slopes s of odd solutions which lie in the invariant torus form two intervals $J_1 \subset I_1$ and $J_2 \subset I_2$, where $J_1 \approx [-3.0266, -3.0247]$. The set $I_1 \setminus \mathrm{Int}(J_1)$ consists of a Cantor type set K_1 and a discrete set D_1. The solutions corresponding to $s \in K_1$ are oscillating and presumably nonquasiperiodic (we computed about 20 oscillations). The solutions corresponding to $s \in D_1$ are asymptotic (i.e. connect the critical points) and are isolated. The set of the limit points of D_1 is exactly K_1. Thus, all oscillating (odd) solutions from K_1 are limits of asymptotic solution with increasing numbers of zero. The set I_2 has a similar structure. Of course our claim is a conjecture based on numerical experiments. We are scanning a certain interval of slopes s with an increment Δs and are looking for local maxima of $x_{max}(s)$. Suppose they are $s_1, s_2, \dots, s_n$. If Δs is sufficiently small we usually did not "jump over" such maxima. Then for each s_i the neighborhood $(s_i - \Delta s, s_i + \Delta s)$ is scanned with smaller Δs_1, say

$\Delta s_1 = \Delta s/400$. If no additional maxima were found, we concluded that there is a unique maxima in the above interval which corresponds to an asymptotic solution. Additional scannings and convergence to the maximum always supported this conclusion. If, however, new maxima were found, their distributions on a smaller scale repeated the distribution of $s_1, s_2, \ldots, s_n$.

The picture described above does not change qualitatively until the invariant torus disappears as c reaches the point P_2. For values of c between P_2 and P_4 both odd periodic solutions are hyperbolic. Here the set I consists of a Cantor type set K and a discrete set D of isolated asymptotic solutions. In general we did not investigate the non-odd bounded solution. However, the presence of non-odd periodic solutions of the branch $P_5P_7'P_8'$ considerably effects the shape of odd bounded solutions. For c between P_7' and P_8', i.e. $0.83645 < c < 0.91695$ the picture is the most interesting. On fig. 3 one can see the projections of 4 periodic orbits on the y, y' plane for $c = 0.85$. The reflection $y \to -y, y' \to y'$ would provide two more non-odd periodic solutions. On figs. 5a–5d we have displayed a typical odd bounded solution for $c = 0.85$ $(x \geq 0)$. The corresponding flame front $v(x)$ on fig. 5d looks completely chaotic. Indeed, numerical experiments with the P.D.E. (1.1) in [6] resulted in flame fronts of the above type. Moreover a closer look on fig. 5a reveals that the trajectory follows closely the periodic orbits for the same value of c. Indeed, three loops around the critical point $y = -\sqrt{2} \approx 1.2$, $y' = 0$ are very close to the periodic solutions 3 and 4 on fig. 3 and to the one on fig. 4d (corresponding to the point P_9'). The large cycle lies near the odd periodic solution #1 on fig. 3 and four loops around the right critical point follow closely the reflected non-odd period solutions. From fig. 5c one can understand the order in which the loops are followed. The small oscillations near -1 correspond to the left centered loops, the one near 1 – to the right centered ones and the simple wave at $88 < x < 95$ corresponds to the large symmetric cycle. On fig. 6a we observe another odd bounded solution for

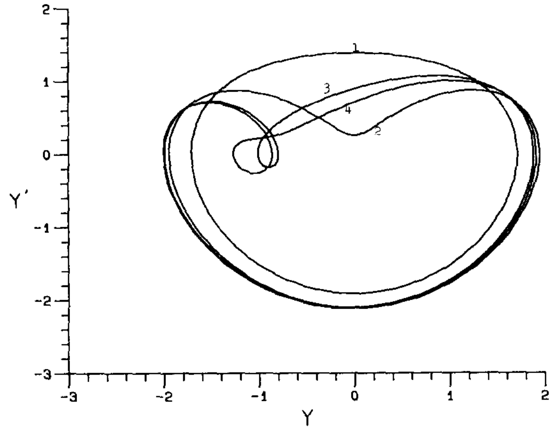

Fig. 3. Periodic solutions at $c = 0.85$: 1-odd solution (right branch of the ω–c curve), 2-odd solution (left branch), 3-nonsymmetric solution (right branch), 4-nonsymmetric solution (left branch).

$c = 0.8$. Observe that the $P_5'P_9'$ curve on fig. 1 crosses the level $c = 0.8$ only once. Hence there is only one non-odd period solution and its reflection, and as a result the trajectory is more trivial. The odd period solution #1 is replaced here by #2. On fig. 6b an odd asymptotic solution (for $x \geq 0$) is displayed. This solution is almost undistinguishable from the one on fig. 6a (their initial slopes differ by 3×10^{-14}!) until it starts to spiral around the critical point. As we already mentioned, in the hyperbolic domains there is a Cantor type set of slopes corresponding to odd oscillating bounded solutions. These bounded solutions follow different combinations of the few periodic orbits. In order to understand which combinations are possible one should study the Poincaré map $\mathscr{P}$ acting in the plane $y'' = 0$. The periodic orbits correspond to the fixed points of $\mathscr{P}$. In the hyperbolic case, there are one dimensional stable and unstable manifolds originating at these points. Apparently these manifolds intersect at heteroclinic or homoclinic points. In the last case it is well known (e.g. see [15]) that there exists an invariant Cantor set in the plane $y'' = 0$ so that $\mathscr{P}$ acts on it as a Bernoulli shift.

We mentioned in the introduction that the branch P_4P_9' on fig. 1 actually continues beyond the point P_9' and terminates as $\omega \to 0$ and $c \to$

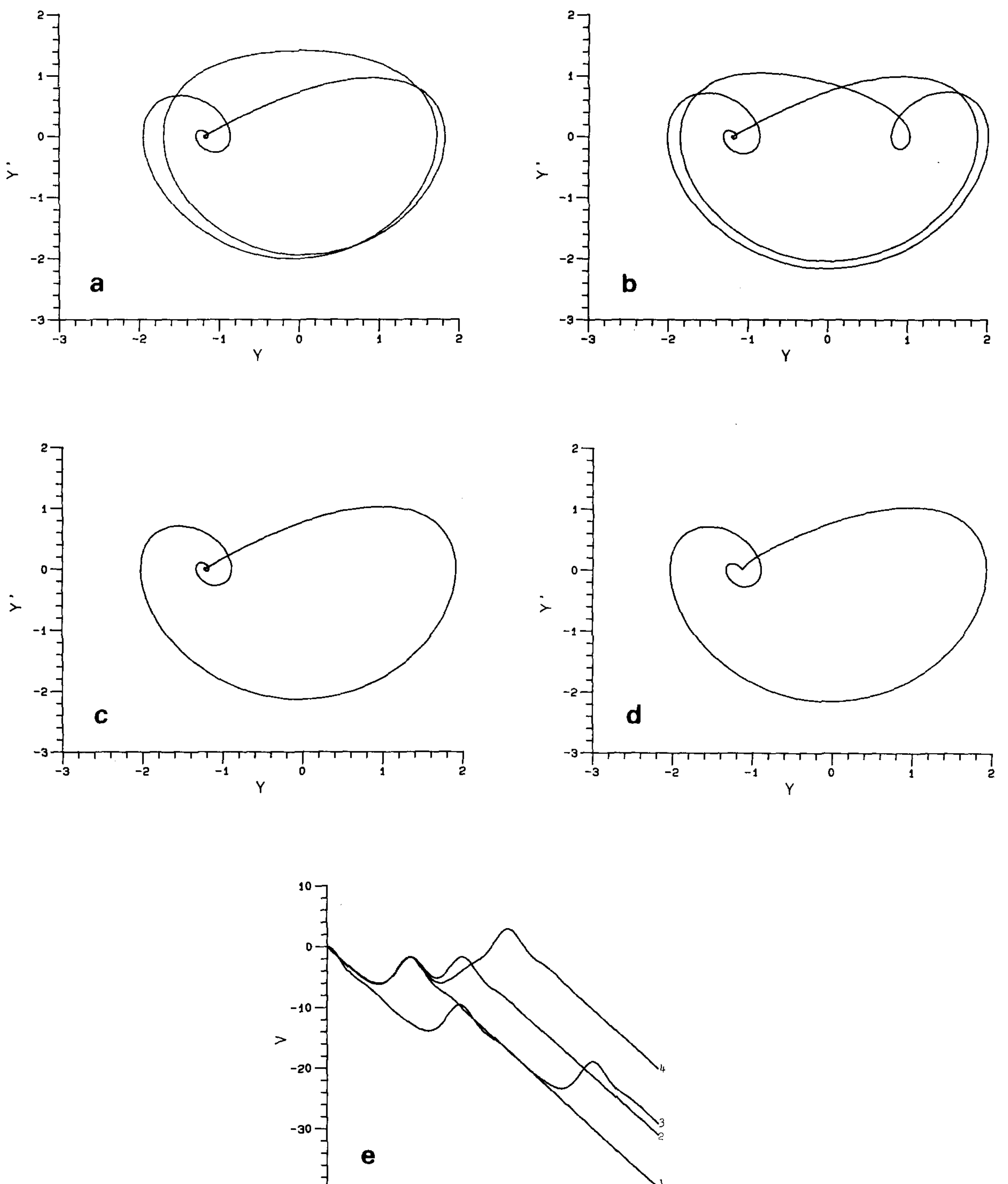

Fig. 4(a) Soliton for $c = \inf C_s \approx 0.835$.(b) Soliton for $c \approx 0.848$. (c) Soliton for $c = \sup C_s \approx 0.86$. (d) Non-symmetric periodic solution at the point $P_9'(c \approx 0.866)$. (e) The flame fronts 1, 2, 3, 4 correspond to figs. 4c, 4a, 4d, 4b.

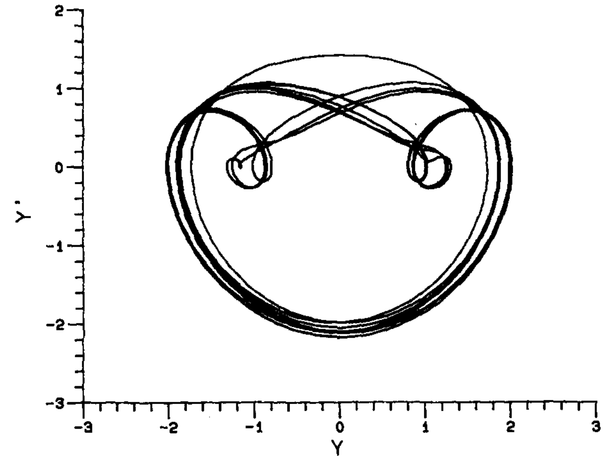

Fig. 5a. One odd "chaotic" solution for $c = 0.85$ (only the part of trajectory for $x \geq 0$ is shown).

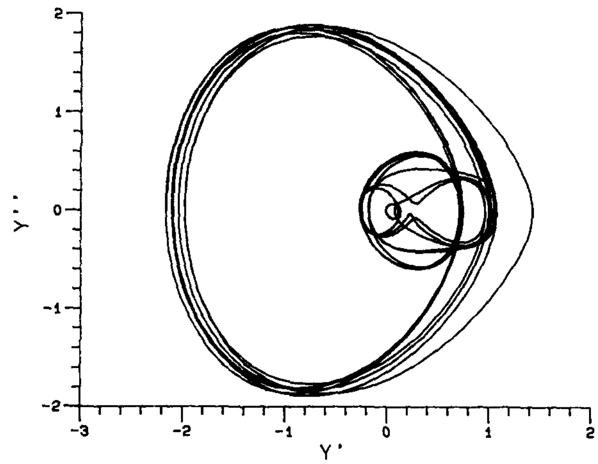

Fig. 5b. The same trajectory as in fig. 5a projected on the $y'y''$ plane.

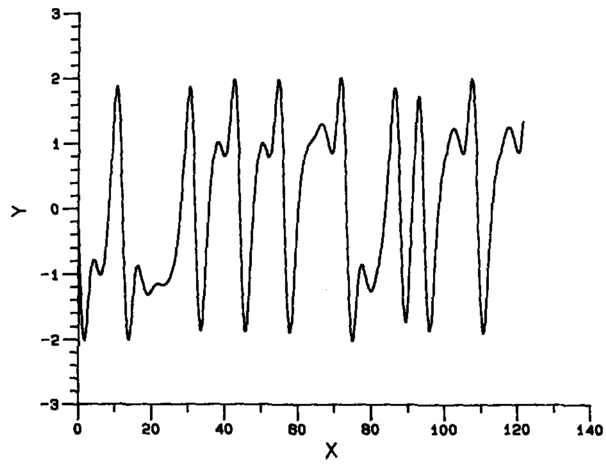

Fig. 5c. The same as in fig. 5a in the x, y plane.

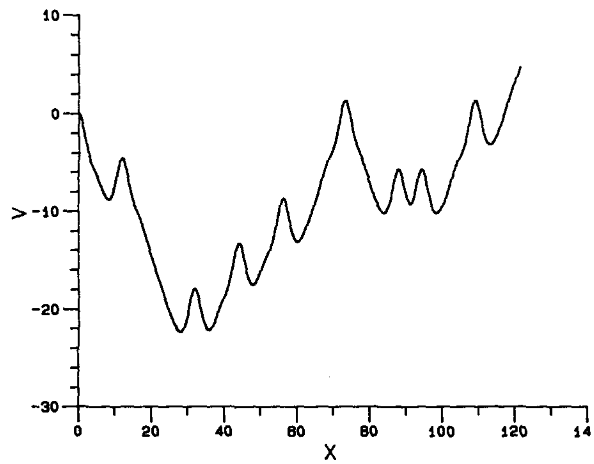

Fig. 5d. Flame front $v(x)$ corresponding to fig. 5a.

≈ 0.86 at the "soliton" displayed on fig. 4c (the name "soliton" is used because $y(x)$ tends to the same limit $c\sqrt{2}$ as $x \to \pm\infty$). Note that the eigenvalues λ_1, λ_2 of the Jacobian $\mathrm{d}\mathscr{P}$ at the periodic orbit tend at the same time to ∞ and 0. Because of it we could not reach beyond the point P_9'. One should mention here an important work of Tzvelodub [8] which only recently came to our attention. Using an entirely different method he obtained the periodic solution for the portions P_0Q and P_4P_9' of fig. 1 (i.e. without the QP_7 part) and followed the P_4P_9' branch until $\omega = 0.06$. He also found the soliton on fig. 4c. It turns out that this i: not the only soliton-like solution. There are i effect two countable sets of values $c' \in C_s \subset [0.835, 0.86]$ and $c \in C_s' \subset [0.48, 0.50]$ for whicl solitons exist! The curve in fig. 4a corresponds t $c = \inf C_s \approx 0.835$, the one of fig. 4b to $c \approx 0.84$ and on fig. 4c to $c = \sup C_s \approx 0.86$. The respectiv oblique flame fronts are shown on fig. 4e. On fig. the two solitons for $c = \inf C_s' \approx 0.4845$ and $c =$ $\sup C_s' \approx 0.49227$ are displayed. Of course a refle tion with respect to the $y = 0$ axis produces anoth soliton which tends to the right critical point. L

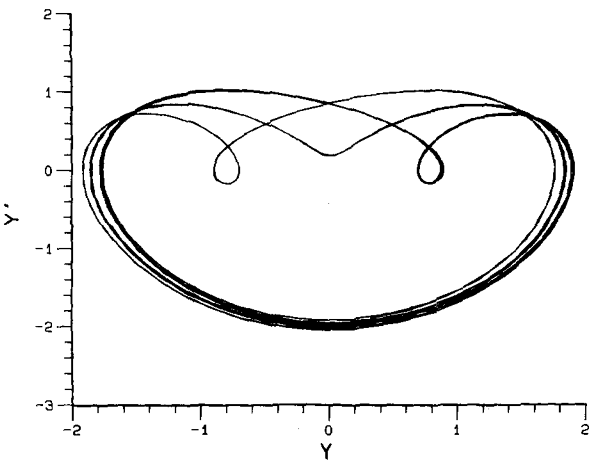

Fig. 6a. One oscilating solution for $c = 0.8$.

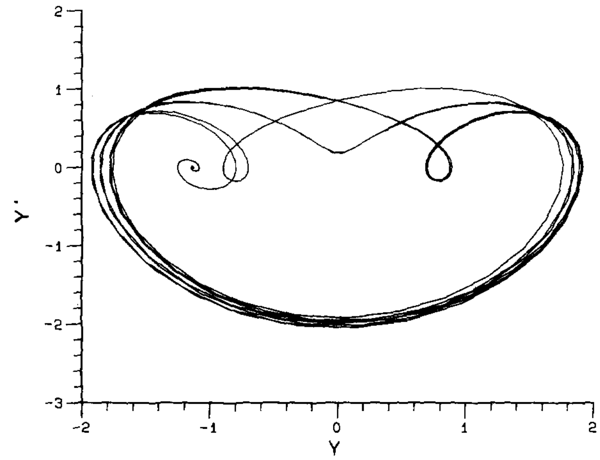

Fig. 6b. An odd asymptotic solution (the half corresponding to $x \geq 0$) for $c = 0.8$.

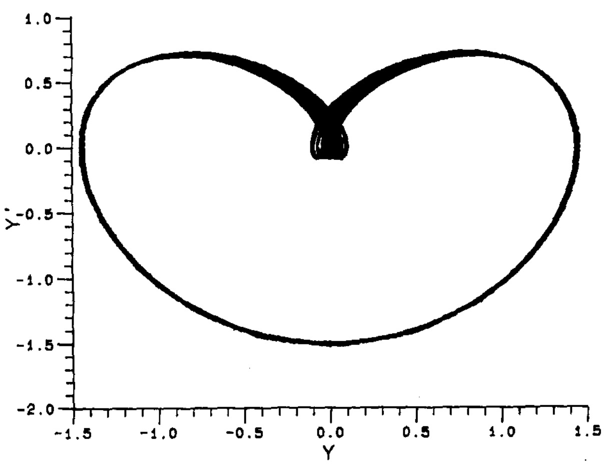

Fig. 7a. $c = 0.59$; Torroidal solution in the elliptic region P_4P_5.

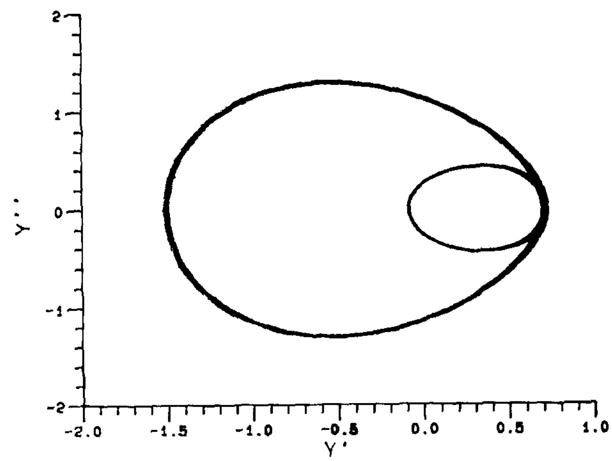

Fig. 7b. The same as in fig. 7a but in the $y'y''$ plane.

us explain in detail how these solitons are found. Each soliton which leaves the left critical point, leaves it by the one-dimensional unstable manifold. Locally this manifold is given by a converging power series. Using this series for the difference scheme (4.1) we compute a triple (y_j, y_{j+1}, y_{j+2}) of points on the unstable manifold and then continue with the scheme (4.1). Let $x_{\max}(c)$ be the first point x where $|y(x)| \geq y_{\max}$. As with the odd solutions we are looking for local maxima of the function $x_{\max}(c)$. It turned out again that these maxima are infinite, i.e. correspond to bounded solutions. Apparently, the respective set of values of c is a Cantor set K_s, while C_s consists of the boundary points of the "holes" of K_s i.e. C_s is the boundary of the complement of K_s. For $c \in K_s \setminus C_s$ the one dimensional unstable manifold wanders in the space around the basic patterns as on figs. 4a–c or fig. 8 and never reaches back the critical point.

In the elliptic domains P_4P_5 and P_6P_7 the left branch periodic solution is surrounded by invariant tori. Two such tori are shown on fig. 7a, b and fig. 9a, b. As we pass through the point

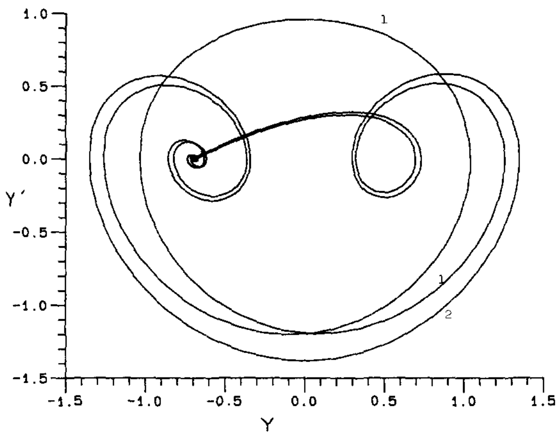

Fig. 8. Two solitons: 1) for $c = \inf C_s' \approx 0.4845$; 2) for $c = \sup C_s' \approx 0.4982$.

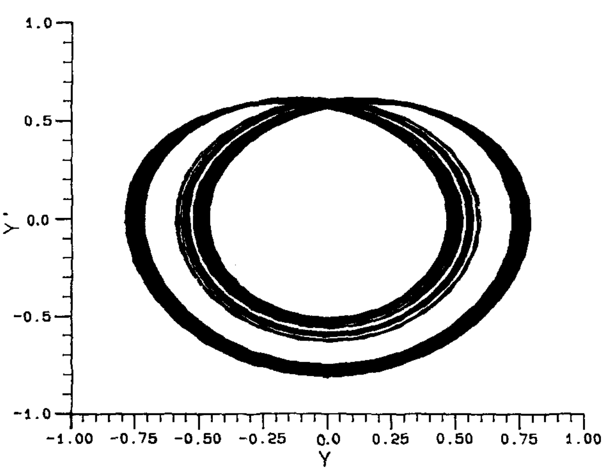

Fig. 9a. $c = 0.33$; Torroidal solution in the elliptic region P_6P_7.

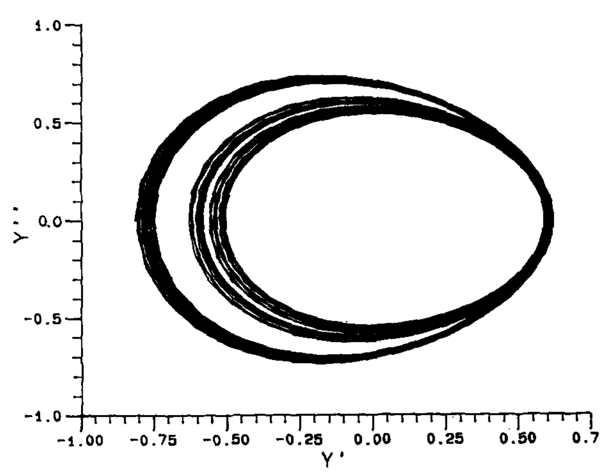

Fig. 9b. The same as in fig. 9a.

$P_7 = P_1$ the maximal torus becomes more and more thick so that for small c it looks as an egg with a narrow hole running from one critical point to another (see fig. 13a, b). One can easily prove that the diameter of the set of bounded solutions tends to zero as $c \to 0$ so that at $c = 0$ the only bounded solution is $y \equiv 0$. An interesting phenomena is displayed on figs. 12a–d. For the same $c = 0.15$ the solution on fig. 12c, d covers densely a torus while the one on fig. 12a, b concentrates in a spiral. It is known [16] that in a vicinity of a fixed elliptic point a measure-preserving map P in a generic situation has homoclinic points which correspond to hyperbolic periodic points of the map The center of the spiral on fig. 12a, b is apparentl such a periodic solution while the spiral has seemingly a Cantor type cross-section caused by presence of a homoclinic point.

At last we should mention the work of Rossle [10]. In particular, Rossler computed some trajec tories of the system

$$\dot{x} = -y - z, \quad \dot{y} = x, \quad \dot{z} = a(y - y^2) - bz.$$

For $b = 0$ this system is equivalent to (1.5) wi $c = a/\sqrt{2}$. On fig. 9. in [10] two trajectories of th

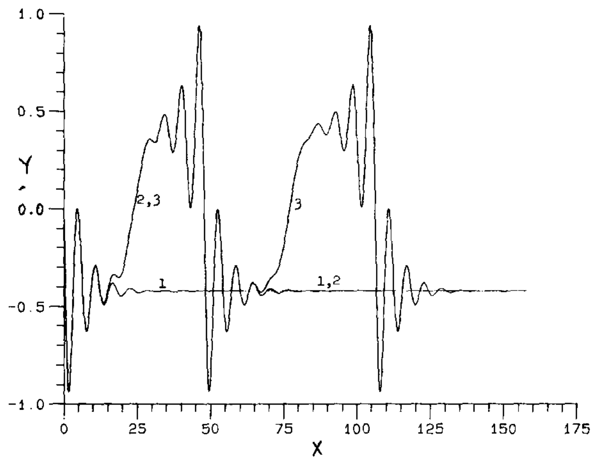

Fig. 10a. $c = 0.3$; Three odd asymptotic solutions: 1) $y^{(0)}$; 2) $y^{(-2)}$; 3) $y^{(-4)}$.

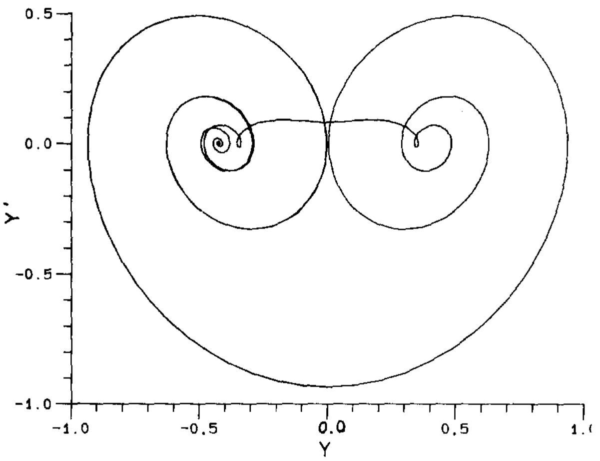

Fig. 10b. Solution $y^{(-2)}$ in the yy' plane.

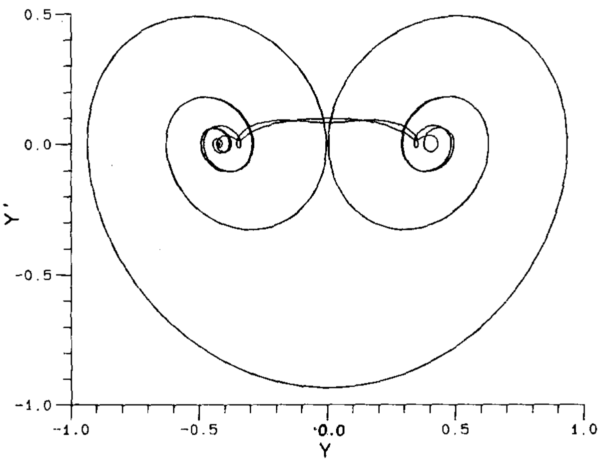

Fig. 10c. Solution $y^{(-4)}$ in the yy' plane.

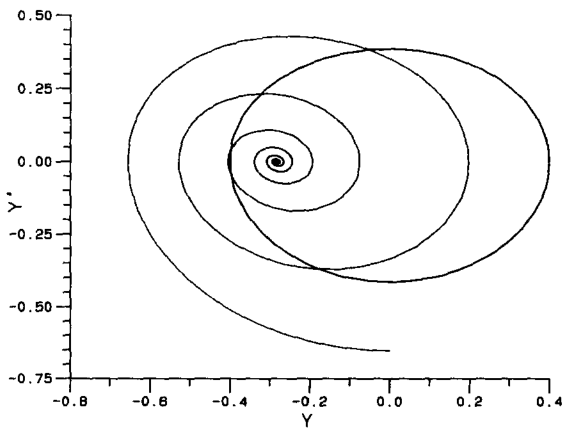

Fig. 11. $c = 0.2$; Asymptotic solution $y^{(0)}$ and a periodic solution.

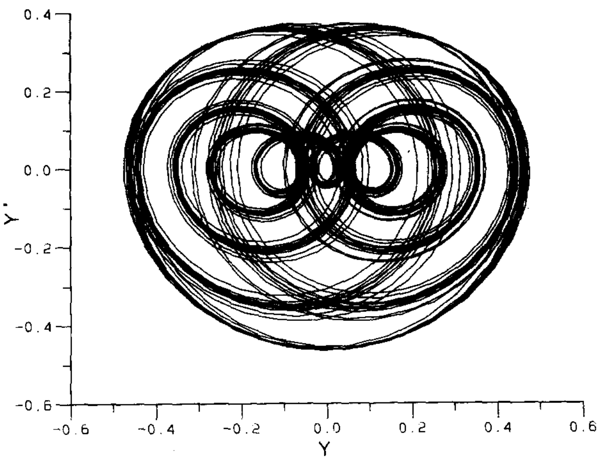

Fig. 12a. $c = 0.15$; A single odd torroidal solution with a slope $y'(0) = -0.464$.

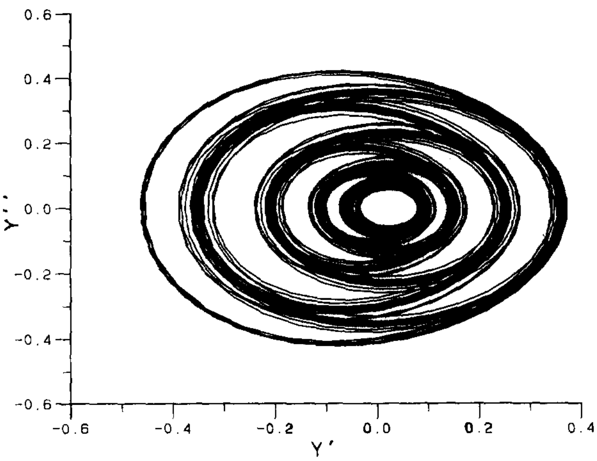

Fig. 12b. The same as in fig. 12a but in the $y'y''$ plane.

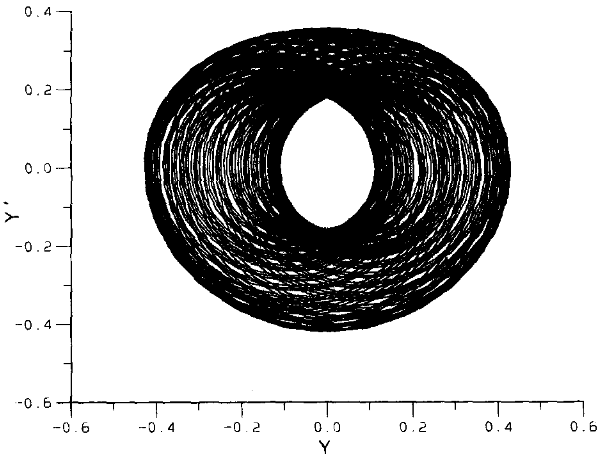

Fig. 12c. $c = 0.15$; analogous to fig. 12a but with a slope $y'(0) = -0.42$.

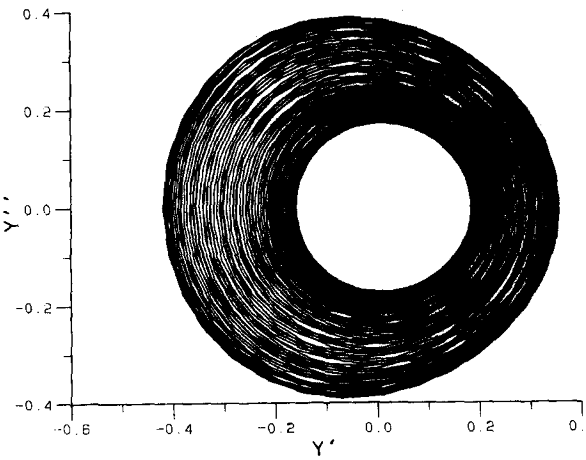

Fig. 12d. The same as in 12c projected on the $y'y''$ plane.

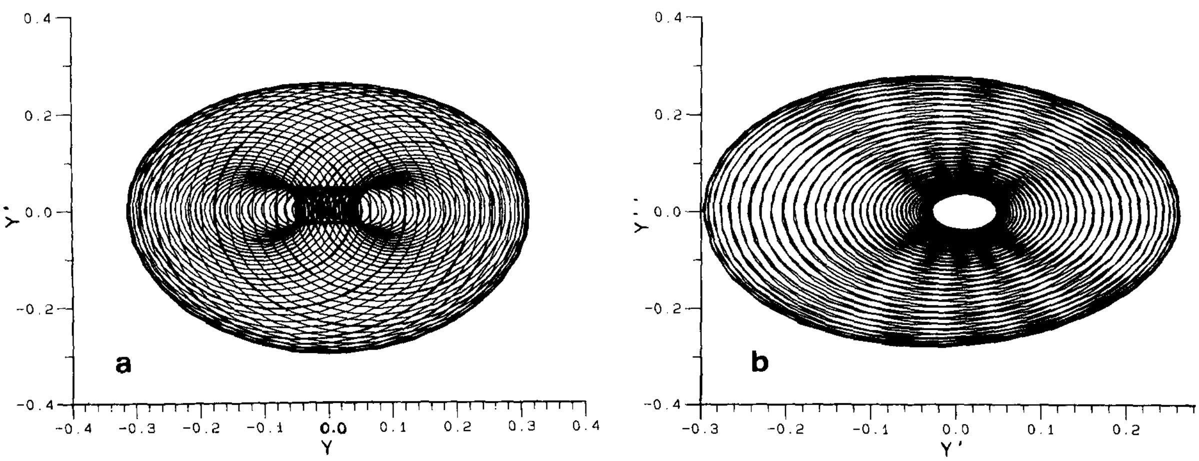

Fig. 13a, b. $c = 0.1$; One torroidal solution.

system are displayed. In the first one $c \approx 0.1414$ and the trajectory lies on a torus. In the second one $c = 0.2828$ and the trajectory after several spirals escapes to infinity. Rossler observes that the invariant tori disappear at $a \approx 0.454$ i.e. $c \approx 0.321$. This indeed agrees with our results.

5. Conclusion

Our analytical and numerical study has shown that the set of steady solutions of the Kuramoto–Sivashinsky equation is surprisingly complex. There are conic solutions which correspond to the Bunsen flames, oblique solitons and waves as well as horizontal periodic, quasi-periodic and chaotic solutions corresponding to a disturbed plane flames. For a high propagation velocity only a single conical solution exists, while for a lower one all the above types of solutions do appear. Our numerical study was devoted mainly to the odd solutions. Certainly, more computations are in place in order to understand the structure of the set of all steady solutions and its dependence on the propagation velocity c^2. However, a more important problem is the connection between the time dependent solutions of (1.1) or (1.6) and the above steady solutions. It was thought previously that the turbulence in the Kuramoto–Sivashinsky equation is primarily of a non-stationary origin and is caused by a competition of a few spatial nodes. In view of the above results it is plausible that the set of steady solutions is an attractor for the time dependent problem. Note that for the (experimental) propagation velocity $c_0^2 \approx 1.2$ of a turbulent flame, both periodic orbits of (1.5) are hyperbolic and there is plenty of spatial chaos in the set of bounded solutions of (1.5). Thus the turbulence in (1.1) may be attributed to the above "steady" chaos. For large c numerical computations suggest that solutions of (1.6) (with proper boundary conditions) tend to the unique conic solution of (1.4). Since the conic solutions are isolated also for small c, it would be interesting to check whether they are locally stable.

Appendix

Here we compute the Poincaré map $\mathscr{P}(\delta z, \delta z'; \varepsilon)$ in (3.40) up to order $\mathcal{O}(\varepsilon^2)$ and the Birkhoff normal form in (3.45).

First we solve the equation

$$z''' + \lambda(\varepsilon) z' = \varepsilon(1 - z^2/2), \quad \lambda(\varepsilon) = 1 = \mathcal{O}(\varepsilon^2) \tag{7.1}$$

in a neighborhood of the periodic solution

$$z_{\text{per}} = -2\sin\xi - \frac{\varepsilon}{6}\sin 2\xi + \mathcal{O}(\varepsilon^2).$$

Expand z as $z = z_{\text{per}} + z_0 + \varepsilon z_1 + \mathcal{O}(\varepsilon^2)$. Then

$$\begin{aligned} &z_0''' + z_0' = 0, \quad z_0 = a_1 + a_2\sin\xi + a_3\cos\xi \\ &z_1''' + z_1' = 2\sin\xi \cdot z_0 - z_0^2/2. \end{aligned} \tag{7.2}$$

Thus

$$\begin{aligned} z_1 = &-a_1\xi\sin\xi + a_2\left(\xi + \frac{1}{6}\sin 2\xi\right) + \frac{a_3}{6}\cos 2\xi \\ &-\frac{1}{2}\left[\left(a_1^2 + \frac{a_2^2 + a_3^2}{2}\right)\xi \right. \\ &\qquad - a_1a_2\xi\sin\xi - a_1a_3\xi\cos\xi \\ &\qquad \left. + \frac{\left(a_3^2 - a_2^2\right)}{12}\cos 2\xi - \frac{a_2a_3}{12}\sin 2\xi\right]. \end{aligned} \tag{7.3}$$

For the Poincaré map we should impose

$$z''(0) = 0 \tag{7.4}$$

and

$$z''(\xi_0) = 0, \quad \text{where } \xi_0 = 2\pi + \Delta\xi. \tag{7.5}$$

Then $\mathscr{P}$ maps $(z(0), z'(0))$ into $(z(\xi_0), z'(\xi_0))$. By (7.4).

$$a_3 = \varepsilon\left(-2a_1 + a_1a_2 - \frac{a_2^2}{6}\right) + \mathcal{O}(\varepsilon^2). \tag{7.6}$$

while by (7.5) and (7.4)

$$\Delta\xi \approx -z''(2\pi)/z'''(2\pi) = \mathcal{O}(\varepsilon^2)/(2-a_2+\mathcal{O}(\varepsilon)) = \mathcal{O}(\varepsilon^2). \tag{7.7}$$

Thus

$$z(\xi_0)-z(0) = z(2\pi)-z(0)+\mathcal{O}(\varepsilon^2) = 2\pi\varepsilon\big(a_2 - a_1^2/2 - a_2^2/4\big)+\mathcal{O}(\varepsilon^2)$$

and

$$z'(\xi_0)-z'(0) = 2\pi\varepsilon(-a_1+a_1a_2/2)+\mathcal{O}(\varepsilon^2).$$

Since $a_1 = z(0)+\mathcal{O}(\varepsilon)$, $a_2 = z'(0)-z'_{\text{per}}(0)+\mathcal{O}(\varepsilon)$, the map $\mathscr{P}$ is given by the formula

$$\mathscr{P}(\delta z,\delta z';\varepsilon) = (\delta z,\delta z') + 2\pi\varepsilon\big(\delta z' - (\delta z)^2/2 - (\delta z')^2/4; -\delta z + \delta z\cdot\delta z'/2\big)+\mathcal{O}(\varepsilon^2). \tag{7.8}$$

where $\delta z = z$, $\delta z' = z' - z'_{\text{per}}(0)$. The differential $\mathrm{d}\mathscr{P}(\varepsilon)$ has two conjugate eigenvalues

$$\lambda = \mathrm{e}^{\mathrm{i}\alpha_0(\varepsilon)},\quad \mu = \bar{\lambda},\quad \alpha_0(\varepsilon) = 2\pi\varepsilon + \mathcal{O}(\varepsilon^2).$$

A linear transformation

$$w = \delta z' + \mathrm{i}\delta z + \mathcal{O}(\varepsilon),\quad \bar{w} = \delta z' - \mathrm{i}\delta z + \mathcal{O}(\varepsilon) \tag{7.9}$$

brings $\mathrm{d}\mathscr{P}(\varepsilon)$ to the diagonal form, while $\mathscr{P}$ becomes

$$\mathscr{P}(w,\bar{w},\varepsilon) = (w_1,\bar{w}_1),$$
$$w_1 = \lambda w + \frac{\mathrm{i}\pi\varepsilon}{8}(-w^2+3\bar{w}^2-6w\bar{w})+\varepsilon^2\mathcal{O}(|w|^2). \tag{7.10}$$

The quadratic transformation

$$w = u + \tfrac{1}{16}(-u^2+6u\bar{u}-\bar{u}^2)+\mathcal{O}(\varepsilon) \tag{7.11}$$

brings $\mathscr{P}$ to the Birkhoff normal form

$$u_1 = \lambda u\,\mathrm{e}^{\mathrm{i}\alpha_1(\varepsilon)u\bar{u}}+\varepsilon^2\mathcal{O}(|u|^3),\quad \alpha_1(\varepsilon) = -\frac{3\pi}{6}\varepsilon+\mathcal{O}(\varepsilon^2). \tag{7.12}$$

With a cubic correction to u of order ε one can reduce the remainder in (7.12) to $\varepsilon^2\mathcal{O}(|u|^4)$.

References

[1] Y. Kuramoto and T. Tsuzuki, Persistent propagation of concentration waves in dissipative media far from thermal equilibrium, Prog. Theor. Phys. 55 (1976) 356–369.

[2] Y. Kuramoto and T. Yamada, Turbulent state in chemical reaction, Prog. Theor. Phys. 56 (1976) 679.

[3] T. Yamada and Y. Kuramoto, A reduced model showing chemical turbulence, Prog. Theor. Phys. 56 (1976) 681.

[4] Y. Kuramoto, Diffusion induced chaos in reaction systems, Suppl. Prog. Theor. Phys. 64 (1978) 346–367.

[5] G. Sivashinsky, Nonlinear analysis of hydrodynamic instability in laminar flames, I. Derivation of basic equations, Acta Astronautica 4 (1977) 1117–1206.

[6] D. Michelson and G. Sivashinsky, Nonlinear analysis of hydrodynamic instability in laminar flames, II. Numerical experiments, Acta Astronautica 4 (1977) 1207–1221.

[7] P. Manneville, Statistical properties of chaotic solutions of a one-dimensional model for phase turbulence, Phys. Lett 84A (1981) 129–132.

[8] O.Yu. Tzverlodub, Stationary travelling waves on a film flowing down an inclined plane, Izvest. Akad. Nauk, Mekh Zhid. Gaza (Russian), No. 4 (1980) pp. 142–146.

[9] T. Mitani, Stable solutions of non-linear flame shape equation, Comb. Science and Technology 36 (1984) 235–247.

[10] O.E. Rossler, Continuous chaos - four prototype equations, Ann. N.Y. Acad. Sci. 316 (1979) 376–392.

[11] O. Thual and U. Frish, Natural boundary in Kuramoto model, presented at the workshop on Combustion, Flame and Fires, March 1–15, 1984, Les Houches.

[12] B. Nicolaenko and B. Scheurer, Remarks on the Kuramoto–Sivashinsky equation, Proceedings of the Conference on Fronts, Interfaces and Patterns, CNLS, Los Alamos, May, 1983, Physica 12D (1984) 391–395.

[13] C. Siegel and J. Moser, Lectures on Celestial Mechanics Grundlehren Bd. 187 (Springer, Berlin, 1971).

[14] J. Moser, On invariant curves of area-preserving mapping of an annulus, Nach. Akad. Wiss. Gottingen, Math. Phy K1 (1962) 1–20.

[15] J. Moser, Stable and Random Motion in Dynamical Systems, with Special Emphasis on Celestial Mechanics (Princeton Univ. Press, Princeton, 1973).

[16] E. Zehnder, Homoclinic points near elliptic fixed points Comm. Pure Appl. Math. 26 (1973) 131–182.

[17] C. Conley, Isolated Invariant Sets and the Morse Index, Conf. Bd. Math. Sci., No. 38 (Amer. Math. Soc., Providence, 1978).

[18] N. Kopell and L.N. Howard, Bifurcations and trajectories joining critical points, Advances in Math. 18 (1975) 306–358.

[19] M.S. Mock, On fourth-order dissipation and single conservation laws, Comm. Pure Appl. Math. 29 (1976) 383–388.

[20] C.K. McCord, Uniqueness of connecting orbits in the equation $y^{(3)} = y^2 - 1$, preprint (Dept. of Math., Univ. of Wisconsin, Madison, 1983).